# Expression of Activated Ras in Gastric Chief Cells of Mice Leads to the Full Spectrum of Metaplastic Lineage Transitions

Eunyoung Choi, Audrey M. Hendley, Jennifer M. Bailey, Steven D. Leach, James R. Goldenring

PII: S0016-5085(15)01735-7
DOI: doi:10.1053/j.gastro.2015.11.049
Reference: YGAST 60179

Published in: *Gastroenterology*

Received date: 30 April 2015
Revised date: 20 November 2015
Accepted date: 24 November 2015

Cite this article as: Choi E, Hendley AM, Bailey JM, Leach SD, Goldenring JR, Expression of Activated Ras in Gastric Chief Cells of Mice Leads to the Full Spectrum of Metaplastic Lineage Transitions, *Gastroenterology*, doi:10.1053/j.gastro.2015.11.049

# Expression of Activated Ras in Gastric Chief Cells of Mice Leads to the Full Spectrum of Metaplastic Lineage Transitions

Eunyoung Choi[1,2], Audrey M. Hendley[5,6], Jennifer M. Bailey[5,6], Steven D. Leach[5,6], and James R. Goldenring[1,2,3,4]

[1]Nashville VA Medical Center, [2]Section of Surgical Sciences and the Epithelial Biology Center, [3]Department of Cell and Developmental Biology, [4]Vanderbilt-Ingram Cancer Center, Vanderbilt University School of Medicine, Nashville, TN 37232

[5]Department of Surgery, [6]The McKusick-Nathans Institute of Genetic Medicine, Johns Hopkins University School of Medicine, Baltimore, MD 21205

**The authors have no conflicts of interest.**

## AUTHOR CONTRIBUTIONS

Choi performed and designed experiments, analyzed data, prepared figures and drafted the manuscript.
Hendley performed and designed experiments and revised the manuscript.
Bailey performed and designed experiments and revised the manuscript.
Leach devised experiments and revised the manuscript.
Goldenring devised experiments and revised the manuscript.

**Address correspondence to:**

James R. Goldenring, MD, PhD
Epithelial Biology Center and Section of Surgical Science
Vanderbilt University Medical Center
10435-G MRB IV
2213 Garland Avenue
Nashville, TN 37232
Tel: 615-936-3726
Fax: 615-343-1591
E-mail: jim.goldenring@vanderbilt.edu

## ABSTRACT

Background & Aims: Gastric cancer develops in the context of parietal cell loss, spasmolytic polypeptide-expressing metaplasia (SPEM), and intestinal metaplasia (IM). We investigated whether expression of the activated form of Ras in gastric chief cells of mice leads to development of SPEM, as well as progression of metaplasia.

Methods: We studied Mist1-CreERT2Tg/+;LSL-K-Ras(G12D)Tg/+ (Mist1-Kras) mice, which express the active form of Kras in chief cells upon tamoxifen exposure. We studied Mist1-CreERT2Tg/+;LSL-KRas (G12D)Tg/+;R26RmTmG/+ (Mist1-Kras-mTmG) mice to examine whether chief cells that express active Kras give rise to SPEM and IM. Some mice received intraperitoneal injections of the MEK inhibitor, selumetinib, for 14 consecutive days. Gastric tissues were collected and analyzed by immunohistochemistry, immunofluorescence, and quantitative PCR.

Results: Mist1-Kras mice developed metaplastic glands, which completely replaced normal fundic lineages and progressed to IM within 3–4 months after tamoxifen injection. The metaplastic glands expressed markers of SPEM and IM, and were infiltrated by macrophages. Lineage tracing studies confirmed that the metaplasia developed directly from Kras (G12D)-induced chief cells. Selumetinib induced persistent regression of SPEM and IM and reestablished normal mucosal cells, which were derived from normal gastric progenitor cells.

Conclusions: Expression of activated Ras in chief cells of Mist1-Kras mice led to the full range of metaplastic lineage transitions, including SPEM and IM. Inhibition of Ras signaling by inhibition of MEK might reverse pre-neoplastic metaplasia in the stomach.

KEY WORDS: carcinogenesis, MAP kinase, differentiation, signal transduction

## ACKNOWLEDGMENTS

We would like to thank Dr. Hideyuki Saya and Dr. Osamu Nagano at Keio University in Japan for providing the anti-CD44v antibody and Dr. Ki Taek Nam (Yonsei University College of Medicine, Korea) for pathology consultation. The authors also wish to thank Dr. Stephen Konieczny for providing Mist1-Cre$^{ERT2}$ mice. These studies were supported by grants from a Department of Veterans Affairs Merit Review Award IBX000930 and NIH RO1 DK071590 and RO1 DK 101332, as well as a grant from the Martell Foundation (to J.R.G), as well as NIH P01 CA134292 and R21 CA158898 (to S.D.L.). Jennifer M. Bailey was also supported by an AACR/Pancreatic Cancer Action Network Pathway to Leadership Award. This work was supported by core resources of the Vanderbilt Digestive Disease Center, (P30 DK058404), the Vanderbilt-Ingram Cancer Center (P30 CA68485, Chemical Synthesis Core), and imaging supported by both the Vanderbilt Combined Imaging Shared Resource and the Vanderbilt Digital Histology Shared Resource.

## INTRODUCTION

Gastric cancer, the second highest cause of cancer-related death in the world,[1] develops in the setting of predisposing mucosal changes including parietal cell atrophy and two metaplastic processes: Spasmolytic polypeptide-expressing metaplasia (SPEM) and intestinal metaplasia (IM).[2-5] Chief cells, a long-lived cell population in the gastric oxyntic glands, represent a cryptic progenitor population, which can give rise to pre-neoplastic metaplasia when induced by the loss of acid-secreting parietal cells, as observed after chronic *Helicobacter* infection.[6] Recent studies in mouse models have demonstrated that SPEM arises from transdifferentiation of chief cells.[6] In humans, increasing evidence suggests that SPEM may then give rise to IM.[3, 7] Investigations in mouse models of *Helicobacter* infection have demonstrated increasing intestinalization of SPEM lineages leading to dysplasia,[8, 9] but these studies have not recapitulated the induction of IM as observed in humans.

While several studies in humans have indicated that SPEM progresses into IM and gastric cancer, the signaling pathways involved in metaplastic transitions remain obscure.[10, 11] Although activating mutations in Ras proteins are common in many epithelial cancers, activating Ras mutations are present in only 10-15% of gastric cancers.[12, 13] Nevertheless, recent profiling studies have noted signatures for activation of Ras activity in at least 40% of gastric cancers.[14, 15] Previous studies have noted hyperplastic and metaplastic changes in the mouse gastric mucosa following global expression of activated Kras, but these mouse models were not able to address the influence of Kras activation in the processes of chief cell transdifferentiation into SPEM or metaplastic progression in the body of the stomach.[16-18]

In this study, we hypothesized that Ras activation in chief cells influences both the induction and progression of metaplasia in the body of the stomach. We have utilized a mouse model, which develops SPEM and IM following induction of active Kras(G12D) expression[19] targeted to chief cells. Induction of active Kras expression in chief cells caused their transdifferentiation into SPEM within a month and progressed to IM over a four-month period. Lineage tracing of chief cells confirmed that the metaplasia developed directly from active Kras induced in chief cells. Thus, induction of active Kras in chief cells leads to the full range of metaplastic changes including both SPEM and IM. Treatment with a MEK inhibitor for two weeks led to the regression of IM and re-establishment of normal mucosal cells. Our results indicate that activation of Ras in chief cells elicits a cascade of metaplastic lineage transitions. Interruption of this process with MEK inhibitors may represent an effective therapeutic approach to reversing metaplasia and preventing gastric carcinogenesis.

## Methods

### Generation of Mist1-Kras, Mist1-Kras-mTmG, Mist1-mTmG mice

The generation of *Mist1-CreERT2*$^{Tg/+}$, *LSL-K-ras(G12D)*$^{Tg/+}$, *R26R*$^{mTmG/+}$ mice has been described previously.[6, 19, 20] All the *Mist1-CreERT2*$^{Tg/+}$, *LSL-K-ras(G12D)*$^{Tg/+}$or *R26R*$^{mTmG/+}$ mice were maintained on a C57BL6 background. *Mist1-CreERT2*$^{Tg/+}$ mice were bred with *LSL-K-ras(G12D)*$^{Tg/+}$ to activate Kras in chief cells. *Mist1-CreERT2*$^{Tg/Tg}$ mice were also bred with *LSL-K-ras(G12D)*$^{Tg/+}$;*R26R*$^{mTmG/+}$ to trace Kras activated chief cells or *R26R*$^{mTmG/+}$ to trace the chief cells. To activate Cre recombinase in *Mist1-CreERT2*$^{Tg/+}$;*LSL-K-Ras(G12D)*$^{Tg/+}$ mice, *Mist1-CreERT2*$^{Tg/+}$;*R26R*$^{mTmG/+}$ mice and *Mist1-CreERT2*$^{Tg/+}$;*LSL-K-Ras(G12D)*$^{Tg/+}$;*R26R*$^{mTmG/+}$ mice, 5 mg of tamoxifen dissolved in corn oil was administered to male and female mice at 8 weeks of age by subcutaneous injection once per day for three consecutive days. Mice were sacrificed 1 week, 1 month, 2 months, 3 months, and 4 months after tamoxifen treatment. The care, maintenance and treatment of the mice used in this study followed protocols approved by the Institutional Animal Care and Use Committees of Vanderbilt University and Johns Hopkins University.

### Selumetinib treatment

Selumetinib (AZD6244) purchased from Selleckchem was dissolved in DMSO to obtain 100 mg/ml of stock solutions and stored at -80 °C. Selumetinib was further diluted from stock solutions to working solutions of 1 mg/ml. To induce IM before Selumetinib treatment, *Mist1-CreERT2*$^{Tg/+}$;*LSL-K-Ras(G12D)*$^{Tg/+}$;*R26R*$^{mTmG/+}$ (Mist1-Kras-mTmG) mice 8 weeks of age were treated with 5 mg of tamoxifen by subcutaneous injection once per day for three consecutive days. After 3 months of tamoxifen treatment, the mice were treated with either DMSO (n=5) or

2 mg/kg of Selumetinib (n=4) by intraperitoneal injection, once per day for 14 consecutive days. All the mice were killed after 1 day after 14 days of treatment. In addition, a group of 3 mice were also treated with Selumetinib for 14 days and then sacrificed 14 days following the last Selumetinib administration (drug recovery).

**Immunohistochemistry and immunofluorescence**

Mouse stomachs from wild type, Mist1-Kras, Mist1-Kras-mTmG, and Mist1-mTmG mice were fixed overnight in 4% paraformaldehyde solution (Affymetrix, 19943) and embedded in paraffin. Paraffin sections (5 μm thickness) were de-paraffinized in Histoclear solution (National Diagnostics, Atlanta, Ga) and hydrated, and antigen retrieval was performed in the Target Retrieval solution (Dako North America, Inc.) using a pressure cooker. After incubating paraffin sections in Protein Block solution (Dako North America, Inc., X0909) at room temperature for 1.5 hours, primary antibodies used for immunohistochemistry and immunofluorescence (Supplementary Table) were incubated at $4^0$C overnight. For immunohistochemistry, the Dako Envision+ System-HRP DAB (Dako North America, Inc.) was used for secondary antibody incubation and DAB development. For immunofluorescence, secondary antibodies conjugated with Cy2, Alexa 488, Cy3, Alexa 555, Alexa 647, Cy5, or Alexa 790 (1:500) were incubated at room temperature for 1 hour. DAPI (1:10,000) was added for nuclear DNA staining in paraffin sections.

**Human samples**

A human tissue array containing SPEM and IM was used for immunohistochemistry with an anti-phosphoERK1/2 antibody and immunofluorescence staining with GSII-Lectin, anti-

phosphoERK1/2 and anti-DMBT1 or anti-Ki67 antibodies. Specimen information of human tissue array described previously. [21, 22]

**Quantitative PCR**

Paraformaldehyde-fixed paraffin-embedded (FFPE) stomach tissue blocks were used to extract total RNAs from the proximal corpus of five Mist1-mTmG mice and six Mist1-Kras mice. Five μm paraffin sections were stained for H&E to identify proximal fundic glands and 2 mm biopsy punches were used to extract the proximal fundic glands. The Qiagen RNeasy FFPE kit was used to extract total RNAs, according to the manufacturer's protocol. One μg of RNA was used for reverse transcription using High-Capacity cDNA Reverse Transcription Kit (Thermo Fisher Scientific). Fresh stomach tissue biopsies were also used to extract total RNAs from proximal corpus of three corn oil control mice and five tamoxifen treated mice using Trizol (Thermo Fisher Scientific) according to the manufacturer's protocol. Samples were analyzed in triplicate and the PCR reactions were performed using EXPRESS SYBR GreenER qPCR SuperMix (Invitrogen). TBP (TATA-box binding protein) gene was used as an endogenous control and the 2-ΔΔCt method was used to compare samples when assessing the expression of the IM markers, such as TFF3, Muc2, Cdx1 and Cdx2. The specific primers used were: TFF3; forward TTGCTGGGTCCTCTGGGATAG and reverse TACACTGCTCCGATGTGACAG, Muc2; forward ACAAAAACCCCAGCAACAAG and reverse GAGCAAGGGACTCTGGTCTG, Cdx1; forward GGACGCCCTACGAATGGATG and reverse TCTTTACCTGCCGCTCTGTGAG, Cdx2; forward GCAGTCCCTAGGAAGCCAAGTGA and reverse CTCTCGGAGAGCCCGAGTGTG, ATP4a; forward TGGCGTGAGGCCTTCCAGACAG and reverse GCGGCATTTGAGCACAGCATCA. Statistical significance ($p<0.05$) was determined by the Mann-Whitney 1-tailed test.

**Immunofluorescence and immunohistochemistry quantitation**

All immunofluorescence images were captured with a Zeiss Axio Imager 2 using a 20X objective. 3 to 5 representative images were captured for each mouse stomach and then the glands of interest for each comparison study were counted and lineage markers were quantitated per gland. For phospho-ERK1/2 and intrinsic factor and/or GSII-Lectin positive or CD44v and Ki67 positive cell counting, labeled cells were counted in 4 images per mouse in a 20× field image. For Clusterin and TFF3-positive cell or Muc2-positive cell counting, labeled cells were counted for 40 to 60 glands per mouse. For GFP -positive cell or Ki-67 and GFP positive cell counting, labeled cells were counted for 30 to 50 glands per mouse. For phospho-ERK1/2-positive cell counting, all stained tissues were scanned using an Ariol SL-50 automated slide scanner at 20X magnification. The phospho-ERK1/2-positive cells were identified and counted only in the entire mucosal area of corpus using Ariol digital analysis. Images were captured at 20X magnification with a resolution of 0.323 μm/pixel. The phospho-ERK1/2-positive cells were identified by upper and lower thresholds for color, saturation and intensity for both blue Hematoxylin staining of nuclei and for brown DAB reaction products. Counted phospho-ERK1/2-positive cell numbers were recorded for each tissue area. Each experimental group contained 3 to 5 mice. Human metaplasia tissue array for metaplastic lesions from the corpus of the stomach [21] were stained with an anti-phospho-ERK1/2 antibody and were imaged on an Ariol SL-50 automated slide scanner (Leica) at 20X magnification. The cores which were positive for phospho-ERK1/2 in the nucleus of mucosal gland cells were considered as phospho-ERK1/2 positive cores. The means, standard deviation, and standard error of the means of quantitation data were generated using Excel. For all comparisons, statistical significance ($P < 0.05$) was calculated using the Mann-Whitney 1-tailed test for two group comparisons and for multiple

comparisons we utilized an ANOVA with post hoc examination of significant means with Bonferroni's test (Prism).

## RESULTS

### Activated Kras expressed in gastric chief cells induces metaplasia.

In the stomach, expression of the transcription factor Mist1 is restricted to zymogen-secreting chief cells.[23] We utilized a Mist1-CreERT2 driver to examine the effects of active Kras induction in chief cells in the *Mist1-CreERT2*$^{Tg/+}$*;LSL-K-Ras(2D)*$^{Tg/+}$ (Mist1-Kras) mouse[24] (Figure 1A). One week after tamoxifen treatment, the stomachs in the Mist1-Kras mouse showed normal oxyntic glands containing parietal cells and chief cells (Figure 1D), as in the normal mucosa in vehicle control and tamoxifen-injected Mist1-CreERT2 control mice (Figure 1D and Supplemental Figure 1). While the glands were negative for Alcian blue (AB) staining (Supplemental Figure 2), phospho-ERK1/2 expression was observed in 15.61±5.65 % of chief cells, indicative of induction of active Kras (Supplemental Figure 3). At four weeks, we observed parietal cell loss, foveolar hyperplasia and SPEM in 94% of the fundic mucosa glands (Figure 1B & C, Supplemental Figure 4). Glands with parietal cells appeared to be compressed towards the basal lamina by expansion of the metaplastic glands (Supplemental Figure 4). However, only one activated caspase-3-positive parietal cell was observed among 60 glands at 4 weeks after tamoxifen treatment, indicating that Kras activation in chief cells does not induce parietal cell apoptosis (Supplemental Figure 5). SPEM cells were positive for PAS staining and weakly-positive for Alcian blue (AB) staining (Supplemental Figure 1B).

The expansion of metaplastic glands evolved into advanced SPEM with intestinalizing characteristics (SPEM-IC) at 2 months after tamoxifen treatment. Stomach sections showed a phenotype similar to the one-month post-treatment stomach (Figure 1D), but 9.6±2.4% of the metaplastic glands showed gland fission (n=8), and also stained strongly for both PAS and AB

(Supplemental Figure 2C). At 3 months after tamoxifen, Mist1-Kras mice developed Goblet cell IM. The strong signals of both PAS and AB were still observed in cells in the base and neck regions of metaplastic glands. Many cells with Goblet morphology were observed in the neck area of the metaplastic glands (Supplemental Figure 2D) and gland fissions were more abundant (18.6±5.1%, n=9) (Figure 1D). Invasive lesions were observed at 4 months post tamoxifen treatment in 13% of mice (n=2/15). The AB staining was significantly decreased in the metaplastic glands at 4 months (Supplemental Figure 2E).

**Characterization of metaplastic glands using SPEM and IM markers.**

To investigate the characteristics of metaplastic glands present, the Mist1-Kras mouse stomachs were co-immunostained with several antibodies against markers of SPEM (Clusterin, GSII-lectin or CD44v) or IM (TFF3 or Muc2). Our previous studies demonstrated that binding of GSII-lectin, which reflects expression of Muc6, and Clusterin are present in normal mucous neck cells, but are strongly upregulated in SPEM.[25-27] To identify glands with SPEM more specifically, we stained for CD44variant 9 (CD44v), a discrete splice variant of the CD44 gene, described as a novel marker for SPEM and early gastric cancer, which is not expressed in the normal body mucosa.[28-30] At one week after tamoxifen treatment, Clusterin and GSII lectin staining was observed only in mucous neck cells, while Intrinsic Factor staining was observed in the chief cells (Figure 2A). No staining for the IM markers, TFF3 or Muc2, was observed in the Mist1-Kras mouse stomachs as expected in a histologically normal gastric mucosa.

At one month after tamoxifen treatment, all of the CD44v-positive metaplastic glands were co-positive for Clusterin and GSII-lectin, confirming that the metaplastic glands were

SPEM (Supplemental Figure 6). Clusterin was observed in the entire area of metaplastic glands and GSII was also observed at the bases of metaplastic glands (Figure 2A). However, the expression of Intrinsic Factor, a marker for chief cells and early SPEM, was dramatically decreased. TFF3, an IM Goblet cell marker, was present in the luminal cells of 88% of the metaplastic glands, which also co-expressed Clusterin (Figure 2B). Muc2, also a Goblet cell marker, was observed in 6% of the metaplastic glands (Figure 2A,C).

At 2 months after tamoxifen treatment, 90% of the metaplastic glands co-expressed clusterin and TFF3 (Figure 2A,B), and Muc2-positive Goblet cells were identified in 13% of the metaplastic glands (Figure 2A,C). At 3 months after tamoxifen treatment, TFF3 was strongly expressed in cells along the entire length of 94% of the glands, with Muc2-positive Goblet cells in 20% of the glands (Figure 2A,B,C). Since Cdx1 is present in human IM [31, 32] and overexpression of Cdx1 induces IM in mouse stomachs,[33] we investigated the expression of Cdx1 in the Mist1-Kras mouse stomachs at 3 months post tamoxifen treatment. We observed nuclear Cdx1 expression in the basal cells of metaplastic glands (Supplemental Figure 7). We did not observe detectable staining for Cdx2 in any metaplastic glands. We also examined the expression of RNA transcripts for IM markers in whole fundic tissue. Muc2 mRNA was significantly increased at 3 months after tamoxifen injection, but TFF3, Cdx1 and Cdx2 mRNAs were not changed in whole tissue (Supplemental Figure 8). These findings suggest that levels of some IM markers may be regulated by post-transcriptional mechanisms. We also stained the Mist1-Kras mouse stomachs at 3 months for PAS and AB and performed transmission electron microscopy to determine whether the TFF3 and Muc2-positive cells truly represented Goblet cells (Figure 2D). The PAS-positive cells contained AB-positive cytoplasmic mucin in a Goblet cell morphology and the electron micrographs showed Goblet cells containing apical mucus

granules (Figure 2D). At 4 months after tamoxifen treatment, Muc2 and TFF3-expressing Goblet cells were mostly confined to the bases of gastric glands (Figure 2A). Interestingly, the basal cells were still positive for all SPEM markers, Clusterin, GSII and CD44v (Supplemental Figure 5), in many glands. These results confirmed that induction of active Kras in chief cells rapidly elicits SPEM, which progresses to IM.

**Metaplastic glands are associated with macrophage infiltrates**

We have recently noted that M2-macrophages promote the progression of SPEM in mouse models and are associated with IM in humans [25]. In Mist1-Kras mice at 4 months after tamoxifen treatment, we observed F4/80-positive cells at the bases of metaplastic glands, which were co-positive for CD163, an M2-macrophage marker (Figure 3A). The CD163-positive M2-macrophages were significantly increased beginning at 2 months after tamoxifen treatment, when the SPEM glands were progressing into IM (Figure 3C). Mist1-Kras mouse stomachs were also immunostained with an antibody against neutrophils, Ly6B.2 (Figure 3B). Similar numbers of Ly6B.2-positive neutrophils were observed in the control and the Mist1-Kras mouse stomachs. These results indicate that M2-macrophages were recruited into the gastric mucosal layer during metaplastic changes in Mist1-Kras mouse stomachs.

**SPEM and IM and are derived from Kras-induced chief cells.**

To examine whether the Mist1-expressing chief cells give rise to the observed metaplastic lineages, we performed lineage tracing from gastric chief cells using *Mist1-*

*CreERT2*$^{Tg/+}$*;LSL-K-Ras(G12D)*$^{Tg/+}$*;R26R*$^{mTmG/+}$ (Mist1-Kras-mTmG) mice (Figure 4A). In the control lineage tracing of gastric chief cells in Mist1-mTmG mice lacking the Kras(G12D) allele, we observed GFP labeling in chief cells of the normal gastric corpus at 1 month after tamoxifen injection (Figure 4B). A minor population of single cells located in the upper neck region of less than 1% of corpus glands was also noted. These cells may represent rare progenitor or pre-pit cells that have some Mist1-trancrtiptional activity. In Mist1-Kras-mTmG mice, we found GFP staining along the entire length of SPEM glands at 1-month post tamoxifen injection (Figure 4B). At 1 week after tamoxifen injection, only 1.4% of GFP-expressing cells stained for Ki67, but 13% of GFP-expressing cells were Ki67-positive at 1 month, indicating that the GFP-expressing glands are more proliferative at 1 month after tamoxifen injection (Supplemental Figure 9). Furthermore, the SPEM and IM lineages also expressed GFP at 2 and 4 months post tamoxifen treatment. These GFP-expressing cells in the metaplastic glands were co-positive for Clusterin, Muc2 and CD44v (Figure 4C), indicating that chief cells expressing active Kras gave rise directly to the metaplastic lineages. Therefore, expression of active Kras in chief cells is sufficient to induce the complete program of lineage changes that lead to SPEM and IM. It should be noted that we did observe gland lineages that expressed clusterin, CD44v, but were negative for GFP, indicating that not all of metaplastic glands derived from Kras-induced chief cells were traced by GFP in Mist1-Kras-mTmG mouse stomachs (Figure 4C). Thus, the two loci for *LSL-K-Ras(G12D)*$^{Tg/+}$ (Kras) and *R26R*$^{mTmG/+}$(mTmG) [20] may respond to the Cre recombinase activity with differing efficiencies, thereby accounting for the presence of metaplastic glands, which are negative for GFP in the Mist1-Kras-mTmG mice. In addition to this likely mosaic activation of the mTmG allele, we are unable to exclude entirely non-cell autonomous recruitment of other cell types in the formation of metaplastic epithelium.

**Inhibition of MEK leads to regression of IM and restoration of normal gastric lineages.**

We performed studies with MEK inhibitor treatment to address whether metaplastic progression can be inhibited by targeting downstream mediators of Kras signaling. We treated Mist1-Kras-mTmG mice at 3 months post tamoxifen treatment, when the mucosa displays prominent IM, either with DMSO vehicle control or a MEK inhibitor, Selumetinib (AZD6244, 2 mg/kg, once daily) for 2 weeks (Figure 5A).[34] The treatment with the MEK inhibitor led to a remarkable regression of metaplasia (Figure 5B). While the metaplastic glands in the DMSO control mouse stomachs were maintained (Figure 5B), the metaplasia in Selumetinib-treated mice was reduced. In addition, normal gastric lineage cells were observed in the glands of mice treated with Selumetinib (Figure 5B).

We also detected reductions in phospho-ERK1/2 staining in the Mist1-Kras mice-treated with Selumetinib (Figure 6). The expression of phospho-ERK1/2 was observed in cell nuclei throughout metaplastic glands in the DMSO-treated mouse stomachs (Figure 6A). We also examined human corpus metaplasia tissue array samples, where over 90% of human SPEM/IM samples showed expression of phospho-ERK1/2 (Supplemental Figure 10), as demonstrated in a previous study.[30] Phospho-ERK1/2 was positive in both SPEM and IM lineages. Additionally, as demonstrated in a serial section, phospho-ERK1/2-positive metaplastic lesions were also co-positive for Ki67, indicating that the phospho-ERK1/2-positive cells were present in proliferating human SPEM lesions and transitional cells between SPEM and IM. However, the expression of phospho-ERK1/2 was significantly decreased in the Selumetinib-treated mouse stomachs (Figure 6B). Many cells in the remaining metaplastic glands in the Selumetinib-treated mouse stomachs

did not express phospho-ERK1/2 and the phospho-ERK1/2 activity decreased 50% in cells of the entire fundic mucosa, compared to DMSO-treated mouse stomachs (Figure 6E). While CD163-positive macrophages were decreased 30% in the Selumetinib-treated mouse stomachs (Supplemental Figure 11), significant M2 macrophage infiltrates were still present.

We also traced GFP-expressing metaplastic glands after Selumetinib treatment to determine the fate of metaplastic cells derived from chief cells. This lineage tracing demonstrated that the DMSO-treated mouse stomachs showed GFP positivity in cells along the entire length of metaplastic glands (Figure 5B). In contrast, the number of GFP-positive cells in metaplastic glands decreased after 2 weeks of Selumetinib treatment (Figure 5B). Interestingly, while the GFP-positive metaplastic cells were relocated towards the surface area, where the phospho-ERK1/2 positive cells remained, GFP-negative normal mucosal cells, including parietal cells, were present in the basal regions of glands in Selumetinib-treated mice (Figure 5B). Thus, GFP-positive metaplastic cells do not give rise to the normal gastric lineage cell types that repopulate the mucosa after Selumetinib treatment.

Additionally, we examined the proliferation of metaplastic cells. We observed a 43% decrease in proliferating metaplastic cells (defined as Ki67+/CD44v+ cells) after Selumetinib treatment. Nevertheless, consistent with a re-establishment of normal gastric lineages, we also observed a 2-fold increase in normal progenitor cell proliferation (defined as Ki67+/CD44v- cells) (Figure 7D). Other normal gastric lineage cells, such as mucous neck cells (CD44v-/GSII+/Intrinsic Factor+) and chief cells (CD44v-/GSII-/Intrinsic Factor+), were also present in the basal regions of glands from Selumetinib-treated mouse stomachs (Figure 5F). These

findings indicate that Selumetinib treatment not only inhibited the progression and proliferation of metaplasia, but also allowed recrudescence of normal gastric lineages.

We finally examined whether the inhibition of the progression and proliferation of metaplasia and re-establishment of normal gastric lineages would persist after withdrawal of Selumetinib treatment. We treated Mist1-Kras-mTmG mice at 3 months post tamoxifen treatment with Selumetinib for 2 weeks, and then analyzed the stomachs of mice 2 weeks following Selumetinib withdrawal (Figure 7A). As in mice actively treated with Selumetinib, 2 weeks after cessation of Selumetinib treatment, the metaplasia was still reduced and normal glands were apparent containing parietal cells and chief cells (Figure 7B). Also, phospho-ERK1/2 expression was prominently reduced even after Selumetinib withdrawal (Figure 6). Interestingly, the AB staining was decreased in the remaining metaplastic glands after Selumetinib withdrawal and many chief cells were clearly observed by H&E staining (Figure 7B). We also traced GFP-expressing metaplastic glands, revealing that the GFP-positive glands were decreased further in the stomachs 2 weeks following Selumetinib withdrawal. The GFP-positive cells were observed in the remaining metaplastic glands, but no GFP-positive cells were found in normal mucosal lineage glands. Instead, parietal cells were observed throughout the glands and chief cells were located at the basal area in the normal mucosal lineage glands (Figure 7C). Moreover, groups of chief cells (CD44v-/GSII-/Intrinsic Factor+) in the basal regions of glands were detected indicating the presence of chief cells differentiated from mucous neck cells (CD44v-/GSII+/Intrinsic Factor-) (Figure 7C). The decrease in proliferating metaplastic cells (as defined as Ki67+/CD44v+ cells) and increase in proliferating normal lineage cells (as defined as Ki67+/CD44v- cells) persisted even after Selumetinib withdrawal (Figure 7C and 7D). These results suggest that even after withdrawal of Selumetinib treatment, re-establishment of normal

gastric lineages continued with replacement of metaplastic glands with glands containing normal lineages.

## DISCUSSION

Chief cells, a long-lived cell population in the gastric oxyntic glands, represent a cryptic progenitor population, which can give rise to pre-neoplastic metaplasia induced by the loss of parietal cells associated with chronic *Helicobacter* infection.[6] In the present investigations, we have described a novel mouse model of metaplasia in the stomach that recapitulates the full range of metaplastic changes including both SPEM and IM.[14, 15, 30]. Previous investigations in mice, including those involving infection with *Helicobacter felis*, have produced SPEM in the body mucosa, but have not shown progression to Goblet cell IM, as is seen in humans.[35, 36] Previous investigations have examined either systemic expression of activated Kras or global expression of activated Kras in the gastric mucosa (e.g. using the K19 promoter).[15-17] While foveolar hyperplasia and metaplasia were observed in the stomach, no systematic analysis of lineage derivation leading to metaplasias was possible. The Mist1-Kras model shows all of the pre-neoplastic stages seen in human gastric carcinogenesis, including transdifferentiation of chief cells into SPEM as an initiation step of metaplastic changes, evolution of SPEM into IM, and development of invasive metaplasia. Since all of these events are driven by induced expression of activated Kras(G12D) exclusively in chief cells, these results also define the transdifferentiation of chief cells as the proximate event in development of metaplastic lesions (Supplemental Figure 12). Moreover, the lineage tracing studies demonstrate that the chief cells are the direct origin of metaplasia and continuing activation of Ras signaling can drive further progression of metaplasia. The success of this model to recapitulate the full metaplastic program likely accrues from the role of Ras activation at all of the key steps. In humans, each of these transitions may involve different candidate agonists of Ras activation. Nevertheless, it is important to note that PANIN lesions do not develop in the Mist1-Kras mouse until 2-3 months

after active Kras induction, suggesting that the earliest stage of metaplasia promotion in the pancreas may not require Ras activation. Unfortunately, we were not able to examine the effect of active Kras expression at longer time points than 4 months after tamoxifen treatment to determine whether this mouse model develops gastric adenocarcinoma, because around 4 months after tamoxifen treatment the mice develop hyperplastic lesions in their salivary glands, which require humane sacrifice. Nevertheless, the progression of metaplastic lesions during the four months of induction suggests that Ras activation may promote all of the critical transitions in the development of pre-neoplastic lesions.

Recent studies have utilized MEK inhibitor treatment for several types of cancer, targeting Kras signaling both in mouse models and human patients.[34, 37, 38] While these studies have focused on treatment of cancers with a high incidence of activating Kras mutations, gastric cancers do not usually harbor Ras mutations. Rather, recent reports have suggested that gastric cancers may have high levels of Ras activation in at least 40% of tumors, due to amplification of upstream signaling pathways.[14, 15] Other investigations have suggested that treatment with a MEK inhibitor may be efficacious in a subset of gastric cancer patients.[39] Our present results suggest for the first time the possibility of using a MEK inhibitor, Selumetinib, as a means to prevent gastric cancer in patients with metaplasia in the stomach by reversing the metaplastic process and allowing the repopulation of the mucosa by normal gastric lineages. The Mist1-Kras-mTmG mouse stomachs showed prominent changes in the metaplastic glands after 2 weeks of Selumetinib treatment. The metaplastic cells were relocated towards the surface area, while normal mucosal cells, such as parietal cells, mucous neck cells and chief cells, were re-established in the basal regions of mucosa. This pattern continued to progress even after withdrawal of Selumetinib treatment. The proliferating metaplastic cells were decreased,

whereas proliferation in the normal progenitor cells was increased. It is important to note that the bases of metaplastic glands were associated with M2-macrophage infiltrates. In the present studies and in more chronic scenarios, macrophages may in turn secrete factors that lead to elevations in epithelial cell Ras activity. Thus, the effects of Selumetinib may arise from blockade of both epithelial and macrophage Ras activities. All of these findings indicate that Selumetinib treatment inhibited the progression of metaplasia, while also allowing recrudescence of normal gastric lineages. Importantly, the lineage tracing study revealed that the emergence of normal gastric lineages following MEK inhibitor treatment was not derived from redifferentiation of metaplastic lineages, but rather accrued from the re-establishment of normal gastric progenitor cells latent within the metaplastic mucosa. Overall, these studies indicate that normal progenitor cells likely lie dormant within the metaplastic mucosa and that, following MEK inhibitor treatment, these cells can regenerate the normal gastric lineage complement causing the extrusion of metaplastic glands from the oxyntic mucosa.

Taken together, our results indicate that expression of active Kras in chief cells can induce their transdifferentiation into SPEM and subsequent development of IM and invasive metaplasia. It is important to note that although eradication of *H. pylori* is routine in patients with Stage I gastric cancer, who undergo endoscopic submucosal resection, these patients maintain a 2-5% per year risk of developing of a second gastric cancer.[40, 41] Thus, therapies that can alter the course of gastric pre-cancer remain a clear priority. Since treatment with a MEK inhibitor could ameliorate the progression of metaplasia in Mist1-Kras mice and also lead to re-establishment of the normal gastric lineages, MEK inhibitor treatment may show efficacy in the treatment of patients with metaplasia and early-stage gastric cancer.

## REFERENCES


1. Parkin DM, Bray FI, Devesa SS. Cancer burden in the year 2000. The global picture. Eur J Cancer 2001;37 Suppl 8:S4-66.
2. Weis VG, Goldenring JR. Current understanding of SPEM and its standing in the preneoplastic process. Gastric Cancer 2009;12:189-97.
3. Goldenring JR, Nam KT, Wang TC, et al. Spasmolytic polypeptide-expressing metaplasia and intestinal metaplasia: time for reevaluation of metaplasias and the origins of gastric cancer. Gastroenterology 2010;138:2207-10, 2210 e1.
4. Goldenring JR, Nomura S. Differentiation of the Gastric Mucosa III. Animal models of oxyntic atrophy and metaplasia. Am J Physiol Gastrointest Liver Physiol 2006;291:G999-G1004.
5. Correa P, Houghton J. Carcinogenesis of Helicobacter pylori. Gastroenterology 2007;133:659-72.
6. Nam KT, Lee HJ, Sousa JF, et al. Mature chief cells are cryptic progenitors for metaplasia in the stomach. Gastroenterology 2010;139:2028-2037 e9.
7. Lennerz JKM, Kim S, Oates EL, et al. The transcription factor MIST1 is a novel human gastric chief cell marker whose expression is lost in metaplasia, dysplasia and carcinoma. . Amer. J. Pathol. 2010;177:1514-1533.
8. Weis VG, Sousa JF, LaFleur BJ, et al. Heterogeneity in mouse SPEM lineages identifies markers of metaplastic progression. Gut 2013;62:1270-1279.
9. Varon C, Dubus P, Mazurier F, et al. Helicobacter pylori Infection Recruits Bone Marrow-Derived Cells That Participate in Gastric Preneoplasia in Mice. Gastroenterology 2012;142:281-91.
10. **Yoshizawa N, Takenaka Y**, Yamaguchi H, et al. Emergence of spasmolytic polypeptide-expressing metaplasia in Mongolian gerbils infected with Helicobacter pylori. Lab Invest 2007;87:1265-1276.
11. Correa P. A human model of gastric carcinogenesis. Cancer Res 1988;48:3554-60.

12. Mita H, Toyota M, Aoki F, et al. A novel method, digital genome scanning detects KRAS gene amplification in gastric cancers: involvement of overexpressed wild-type KRAS in downstream signaling and cancer cell growth. BMC Cancer 2009;9:198.
13. Holbrook JD, Parker JS, Gallagher KT, et al. Deep sequencing of gastric carcinoma reveals somatic mutations relevant to personalized medicine. J Transl Med 2011;9:119.
14. Deng N, Goh LK, Wang H, et al. A comprehensive survey of genomic alterations in gastric cancer reveals systematic patterns of molecular exclusivity and co-occurrence among distinct therapeutic targets. Gut 2012;61:673-84.
15. Network TCGAR. Comprehensive molecular characterization of gastric adenocarcinoma. Nature 2014;513:202-9.
16. Matkar SS, Durham A, Brice A, et al. Systemic activation of K-ras rapidly induces gastric hyperplasia and metaplasia in mice. Am J Cancer Res 2011;1:432-445.
17. Ray KC, Bell KM, Yan J, et al. Epithelial tissues have varying degrees of susceptibility to Kras(G12D)-initiated tumorigenesis in a mouse model. PLoS One 2011;6:e16786.
18. **Okumura T, Ericksen RE**, Takaishi S, et al. K-ras mutation targeted to gastric tissue progenitor cells results in chronic inflammation, an altered microenvironment, and progression to intraepithelial neoplasia. Cancer Res 2010;70:8435-45.
19. Johnson L, Mercer K, Greenbaum D, et al. Somatic activation of the K-ras oncogene causes early onset lung cancer in mice. Nature 2001;410:1111-6.
20. Muzumdar MD, Tasic B, Miyamichi K, et al. A global double-fluorescent Cre reporter mouse. Genesis 2007;45:593-605.
21. Leys CM, Nomura S, Rudzinski E, et al. Expression of Pdx-1 in human gastric metaplasia and gastric adenocarcinoma. Hum Pathol 2006;37:1162-8.
22. Leys CM, Nomura S, LaFleur BJ, et al. Expression and prognostic significance of prothymosin-alpha and ERp57 in human gastric cancer. Surgery 2007;141:41-50.

23. Ramsey VG, Doherty JM, Chen CC, et al. The maturation of mucus-secreting gastric epithelial progenitors into digestive-enzyme secreting zymogenic cells requires Mist1. Development 2007;134:211-22.

24. **Habbe N, Shi G**, Meguid RA, et al. Spontaneous induction of murine pancreatic intraepithelial neoplasia (mPanIN) by acinar cell targeting of oncogenic Kras in adult mice. Proc Natl Acad Sci U S A 2008;105:18913-8.

25. Petersen CP, Weis VG, Nam KT, et al. Macrophages Promote Progression of Spasmolytic Polypeptide-Expressing Metaplasia Following Acute Loss of Parietal Cells. Gastroenterology 2014.

26. Weis VG, Sousa JF, LaFleur BJ, et al. Heterogeneity in mouse spasmolytic polypeptide-expressing metaplasia lineages identifies markers of metaplastic progression. Gut 2012;62:1270-9.

27. Kang W, Rathinavelu S, Samuelson LC, et al. Interferon gamma induction of gastric mucous neck cell hypertrophy. Lab Invest 2005;85:702-15.

28. **Wada T, Ishimoto T**, Seishima R, et al. Functional role of CD44v-xCT system in the development of spasmolytic polypeptide-expressing metaplasia. Cancer Sci 2013;104:1323-9.

29. Hirata K, Suzuki H, Imaeda H, et al. CD44 variant 9 expression in primary early gastric cancer as a predictive marker for recurrence. Br J Cancer 2013;109:379-86.

30. Khurana SS, Riehl TE, Moore BD, et al. The hyaluronic acid receptor CD44 coordinates normal and metaplastic gastric epithelial progenitor cell proliferation. J Biol Chem 2013;288:16085-97.

31. Niwa T, Ikehara Y, Nakanishi H,et al. Mixed gastric- and intestinal-type metaplasia is formed by cells with dual intestinal and gastric differentiation. J Histochem Cytochem 2005;53:75-85.

32. Almeida R, Silva E, Santos-Silva F,et al. Expression of intestine-specific transcription factors, CDX1 and CDX2, in intestinal metaplasia and gastric carcinomas. J Pathol 2003;199:36-40.

33. Mutoh H, Sakurai S, Satoh K, et al. Cdx1 induced intestinal metaplasia in the transgenic mouse stomach: comparative study with Cdx2 transgenic mice. Gut 2004;53:1416-23.

34. Chen Z, Cheng K, Walton Z, et al. A murine lung cancer co-clinical trial identifies genetic modifiers of therapeutic response. Nature 2012;483:613-7.

35. Wang TC, Goldenring JR, Dangler C, et al. Mice lacking secretory phospholipase A2 show altered apoptosis and differentiation with Helicobacter felis infection. Gastroenterology. 1998;114:675-689.

36. Fox JG, Li X, Cahill RJ, et al. Hypertrophic gastropathy in Helicobacter felis-Infected wild type C57BL/6 mice and p53 hemizygous transgenic mice. Gastroenterology. 1996;110:155-166.

37. Larkin J, Ascierto PA, Dreno B, et al. Combined Vemurafenib and Cobimetinib in BRAF-Mutated Melanoma. N Engl J Med 2014; [Epub ahead of print].

38. Dankort D, Filenova E, Collado M, et al. A new mouse model to explore the initiation, progression, and therapy of BRAFV600E-induced lung tumors. Genes Dev 2007;21:379-84.

39. **Sogabe S, Togashi Y**, Kato H, et al. MEK inhibitor for gastric cancer with MEK1 gene mutations. Mol Cancer Ther 2014;13:3098-106.

40. Pimentel-Nunes P, Mourao F, Veloso N, et al. Long-term follow-up after endoscopic resection of gastric superficial neoplastic lesions in Portugal. Endoscopy 2014;46:933-40.

41. Kosaka T, Endo M, Toya Y,et al. Long-term outcomes of endoscopic submucosal dissection for early gastric cancer: a single-center retrospective study. Dig Endosc 2014;26:183-91.

## FIGURE LEGENDS

**Figure 1. Mist1Cre-mediated active Kras expression in chief cells.** A) Experimental strategy of Cre-mediated recombination in the (Mist1-Kras) mouse stomachs. Active Kras(G12D) expression was induced after STOP cassette excision by tamoxifen treatment. B) Histological staining of the stomachs of Mist1-Kras mice. Sections from Mist1-Kras mouse stomachs at 1 month post vehicle control or tamoxifen (induced) injection were examined by hematoxylin and eosin (H&E) staining. Dotted boxes indicate regions enlarged. C) 150 glands in the proximal region of corpus were examined in each group (n=7). 94.76% of glands showed parietal cells loss and SPEM. D) Key metaplastic stages were defined after active Kras induction. Data are representative of n = 3 mice for 1 week time point and n = 10 to15 mice per time point between 1 and 4 months. Dotted boxes denote regions enlarged in the second row. Scale bars are 100 μm.

**Figure 2. Development of metaplasia in the Mist1-Kras mouse.** A) Co-immunostaining for various SPEM and IM markers in the corpus of stomach sections from mice corn oil control, 1 week and 1 to 4 months post tamoxifen treatment (n=3). Clusterin (green) was observed in the mucous neck cells in corn oil control mouse stomachs and at 1-week post tamoxifen treatment, and also in SPEM or IM cells beginning at 1 month post tamoxifen treatment. TFF3 (red) was observed in the metaplastic glands beginning at 1 month. Intrinsic factor (IF, red) and GSII-Lectin (GSII, gray)-positive cells indicate SPEM. Muc2-positive Goblet cells (green) were present in the middle of metaplastic glands beginning at 2 months post tamoxifen treatment (white arrows). B) Quantitation of immunohistochemical analysis of SPEM (Clusterin) and/or IM (TFF3) marker-expressing glands in Mist1-Kras mouse stomachs from 1 to 4 months. C)

Quantitation of immunochemical analysis of glands with Muc2-positive Goblet cells in Mist1-Kras mouse stomachs from control (0) to 4 months. ∗ = p< 0.05. D) Sections from Mist1-Kras mouse stomachs at 3 months after tamoxifen injection were examined by periodic acid–Schiff (PAS) or Alcian blue staining (AB). Transmission electron micrograph of the metaplastic glands showing Goblet cells filled with mucus granules. 6500x. Boxes indicate regions enlarged. Scale bars = 100 μm.

**Figure 3. Immunofluorescence staining of macrophage markers in Mist1-Kras mouse stomachs.** A and B) Corpus regions from uninduced wild type mouse stomachs (control) or Mist1-Kras mouse stomachs (Mist1-Kras) at 4 months post tamoxifen treatment were co-immunostained with antibodies against macrophage M2 marker, CD163 (green), and macrophage and dendritic cell marker, F4/80 (red) (A) or with antibodies against neutrophil and polymorphonuclear cell marker, Ly6B.2 (red), and GSII-lectin (B). The F4/80-positive macrophages were observed in the Mist1-Kras mouse stomachs and were co-positive for CD163 (white arrow). The Ly6B.2-positive neutrophils were observed both in the control and the Mist1-Kras mouse stomachs. DAPI was used for nuclear staining (blue). Dotted box indicates regions enlarged. Scale bars = 100 μm. * = p<0.05. C) CD163-positive macrophages were counted per 20X field of images taken in the corpus from corn oil control, 1 week, and 1 to 4 months after tamoxifen treatment (n=3 to 4). * = p<0.05.

**Figure 4. Lineage mapping of Cre-induced chief cells in Mist1-mTmG and Mist1-Kras-mTmG mice.** A) Experimental strategy of Cre-mediated recombination in the Mist1-Kras-mTmG mouse stomachs. The *R26R*$^{mTmG/+}$ allele expresses red fluorescent protein in the membrane prior to Cre recombinase-mediated excision (mT). However, after Cre-dependent excision, cells express green fluorescent protein in the membrane (mG). B) Immunohistochemistry for GFP in stomach sections of control Mist1-mTmG mice (no Kras) or Mist1-Kras-mTmG mice. C) The GFP (+) metaplastic glands in the corpus were co-immunostained with antibodies against Clusterin, Muc2, or CD44v from Mist1-Kras-mTmG mouse stomachs at 2 months after tamoxifen injection. DAPI was used for nuclear staining. Boxes indicate regions enlarged. Scale bars = 100 μm.

**Figure 5. Regression of Kras-induced metaplasia by MEK inhibition.** A) Selumetinib treatment schematic. At 3 months post tamoxifen treatment, Mist1-Kras-mTmG mice were treated with either DMSO (n=5) or 2 mg/kg Selumetinib (n=4) once daily for 2 weeks. B) Top row: H&E stained stomachs from mice treated with DMSO or with Selumetinib. DMSO treated mice showed severe metaplasia (arrow), but normal mucosal cells were observed in glands of Selumetinib-treated mice (arrows). Sections of the corpus from DMSO or Selumetinib treated mouse stomachs were immunostained with antibodies against GFP (green) and H/K-ATPase (red) (middle row) or with antibodies against CD44v (green), Ki67 (red) and intrinsic factor (blue), and GSII-lectin (white) (bottom row). DAPI was used for nuclear staining. Mucous neck cells (GSII+/CD44v-, white arrow) and chief cells (IF+/CD44v-, yellow arrow) were also observed in the Selumetinib-treated mice. Yellow dotted lines indicate the junction of zones between

proliferating metaplastic cells and normal progenitor cells. Boxes indicate regions enlarged. Scale bars = 100 μm.

**Figure 6. Immunohistochemistry of phospho-ERK1/2 in Selumetinib treated mouse stomachs.** Sections of the fundic glands from Mist1-Kras-mTmG mice treated at 3 months after tamoxifen treatment with DMSO, Selumetinib-treated, or 2 weeks post Selumetinib treatment and wild type mouse (control) were examined for phospho-ERK1/2 immunostaining. A) The stomachs from Mist1-Kras-mTmG mice treated with DMSO showed strong phospho-ERK1/2 staining throughout the metaplastic glands. The stomachs from Mist1-Kras-mTmG mice treated with Selumetinib (B) or at 2 weeks post Selumetinib treatment (C) showed decreases in phospho-ERK1/2 compared to the DMSO treated mice. D) In the control mouse stomachs, phosphorylation of ERK1/2 was occasionally observed in the foveolar or progenitor cells in the neck region. Boxes indicate regions enlarged. Scale bars = 100 μm. E) The phospho-ERK1/2 (+) cells were counted in all mucosal areas of corpus from DMSO- (n=5), Selumetinib-treated (n=4) or at 2 weeks post Selumetinib treatment (n=3) mice. *$p < 0.05$.

**Figure 7. Continued re-establishment of normal gastric lineages after Selumetinib withdrawal.** A) Selumetinib treatment schematic. At 3 months after tamoxifen treatment, Mist1-Kras-mTmG mice were examined at the end of 2 weeks of Selumetinib treatment (n=4) or two weeks following cessation of Selumetinib (n=3). B) H&E stained stomachs from mice treated with Selumetinib or 2 weeks post Selumetinib treatment. C) Sections of the corpus from the mouse stomachs 2 weeks after cessation of Selumetinib treatment were immunostained with

antibodies against GFP (green), H/K-ATPase (red), DAPI (white) and IF (blue) (top row), or against IF (green), CD44v (red), DAPI (blue) and GSII-lectin (white) (middle row), or against CD44v (green), Ki67 (red) and GSII-Lectin (blue) (bottom row). Several mucous neck cells (GSII+/CD44v-, white arrows) and chief cells (IF+/CD44v-, yellow arrows) were observed. Boxes indicate regions enlarged. Scale bars = 100 μm. D) Quantitation of proliferating cells in Selumetinib-treated Mist1-Kras-mTmG mouse stomachs. Two classes of Ki67-positive cells, Normal proliferating cells (Ki67+/CD44v-) and Metaplastic proliferating cells (Ki67+/ CD44v+), were counted in glands in the corpus from DMSO- (n=5) or Selumetinib-treated (n=4), or 2 weeks post Selumetinib-treated (n=3) mouse stomachs. *$p<0.05$.

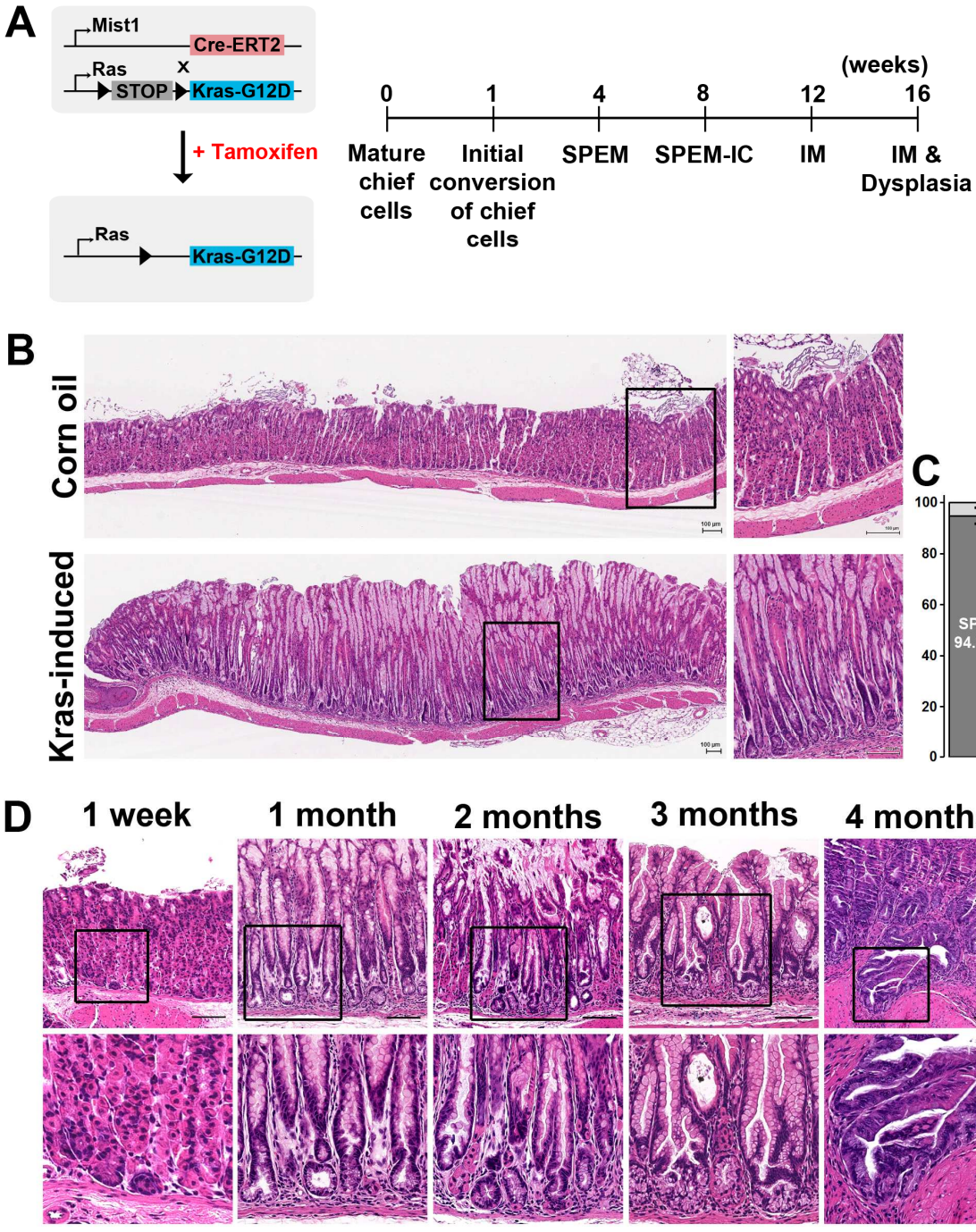
A
Mist1
Cre-ERT2
Ras
STOP
x
Kras-G12D
+ Tamoxifen
Ras
Kras-G12D
(weeks)
0
1
4
8
12
16
Mature chief cells
Initial conversion of chief cells
SPEM
SPEM-IC
IM
IM & Dysplasia
B
Corn oil
Kras-induced
C
100
80
60
40
20
0
SPEM
94.76%
D
1 week
1 month
2 months
3 months
4 months

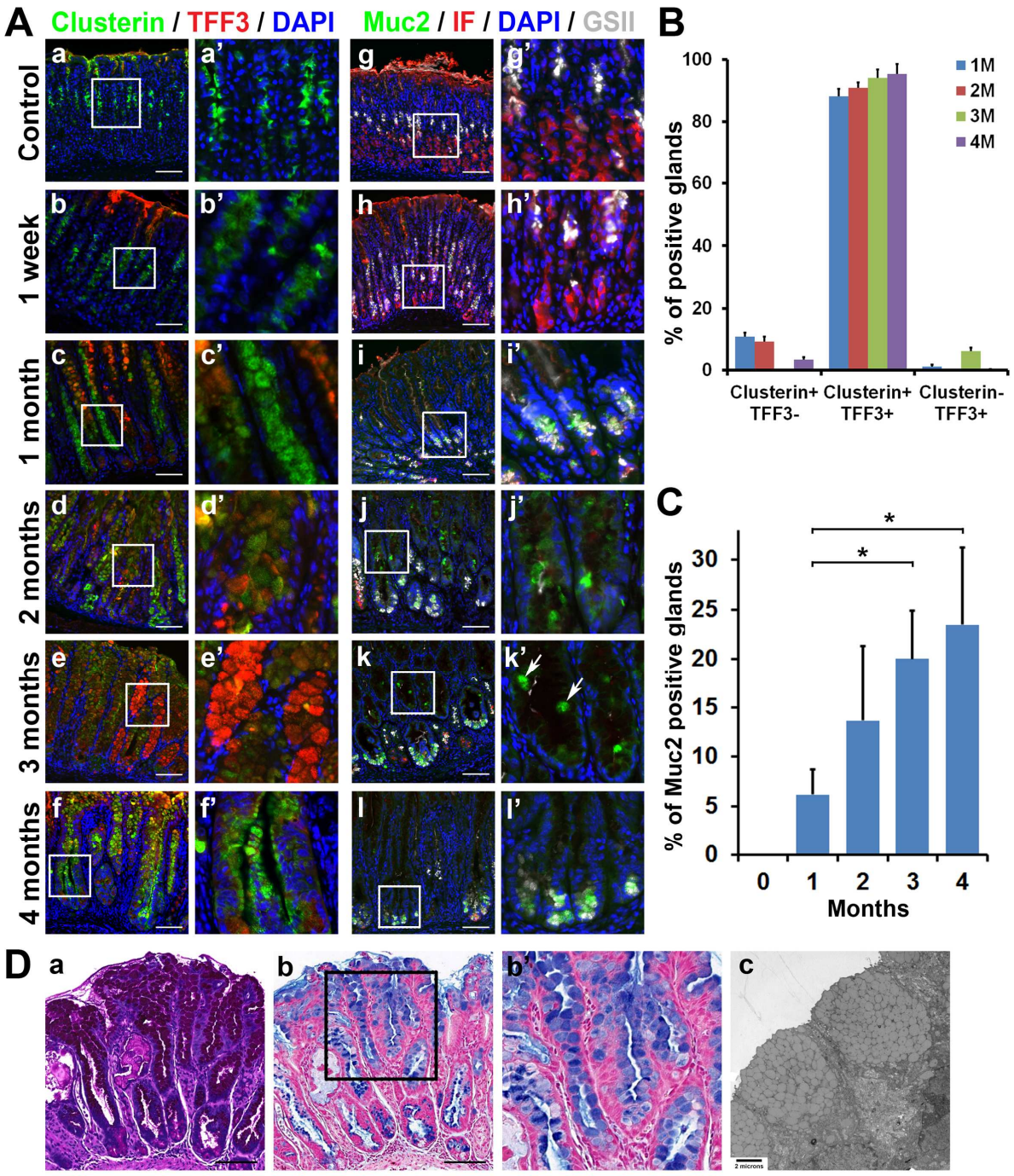
A
Clusterin / TFF3 / DAPI
Muc2 / IF / DAPI / GSII
Control
1 week
1 month
2 months
3 months
4 months
a
a'
g
g'
b
b'
h
h'
c
c'
i
i'
d
d'
j
j'
e
e'
k
k'
f
f'
l
l'
B
% of positive glands
100
80
60
40
20
0
1M
2M
3M
4M
Clusterin+ TFF3-
Clusterin+ TFF3+
Clusterin- TFF3+
C
% of Muc2 positive glands
30
25
20
15
10
5
0
*
*
0
1
2
3
4
Months
D
a
b
b'
c
2 microns

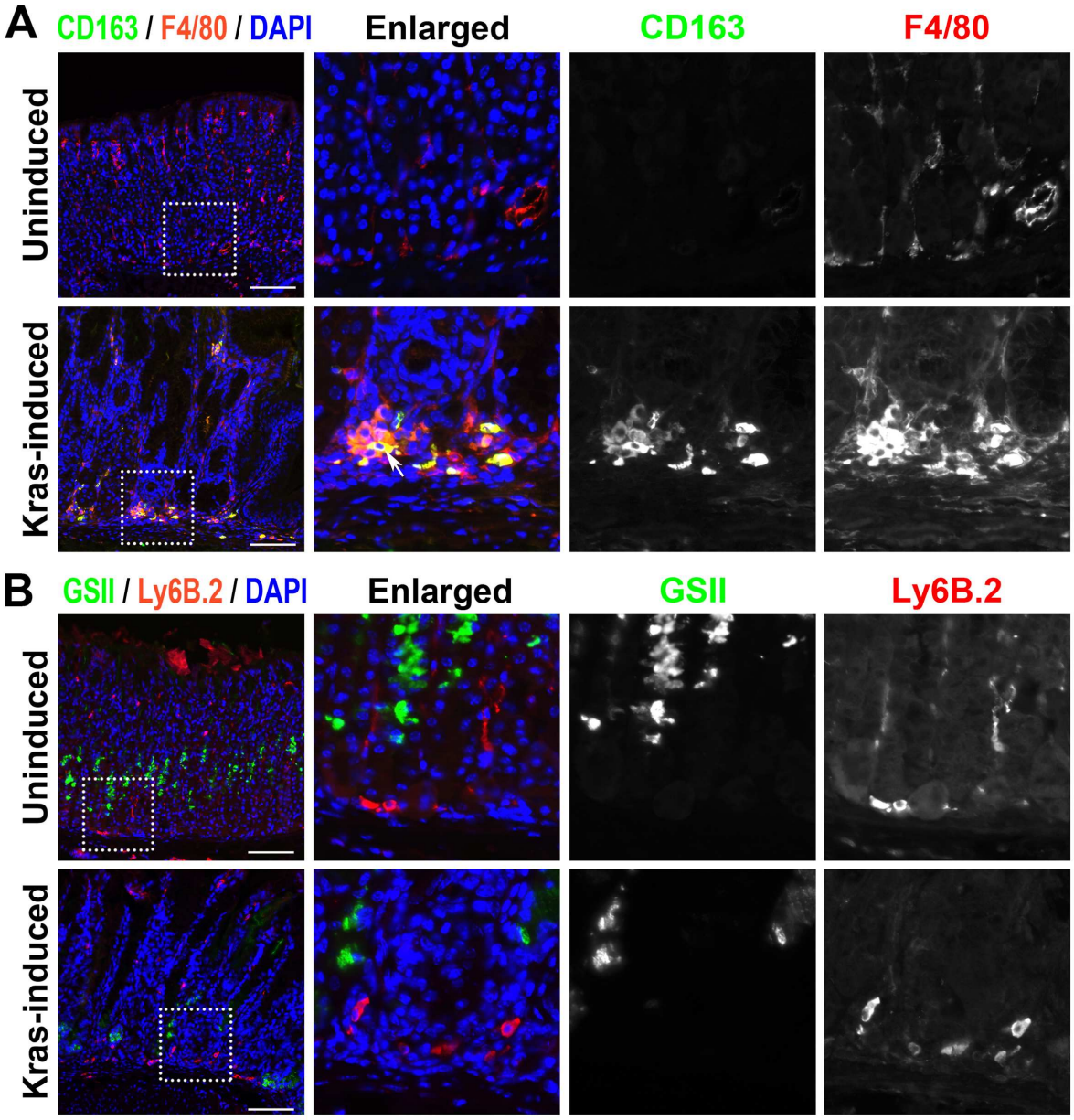
A
CD163 / F4/80 / DAPI
Enlarged
CD163
F4/80
Uninduced
Kras-induced
B
GSII / Ly6B.2 / DAPI
Enlarged
GSII
Ly6B.2
Uninduced
Kras-induced

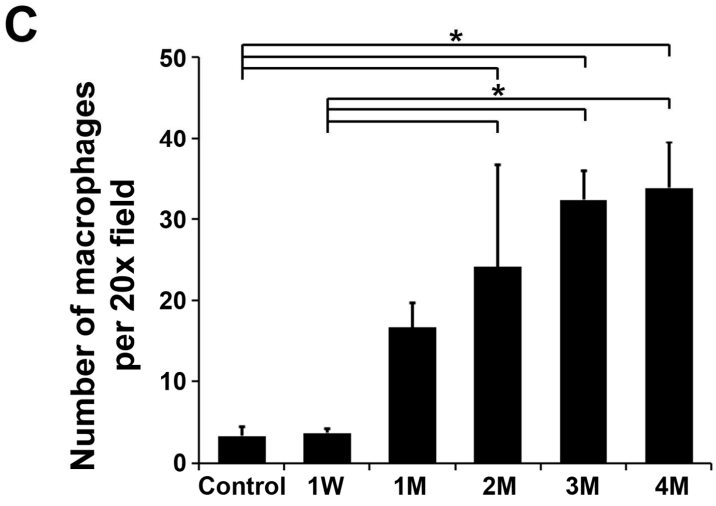
C
Number of macrophages per 20x field
0
10
20
30
40
50
*
*
Control
1W
1M
2M
3M
4M

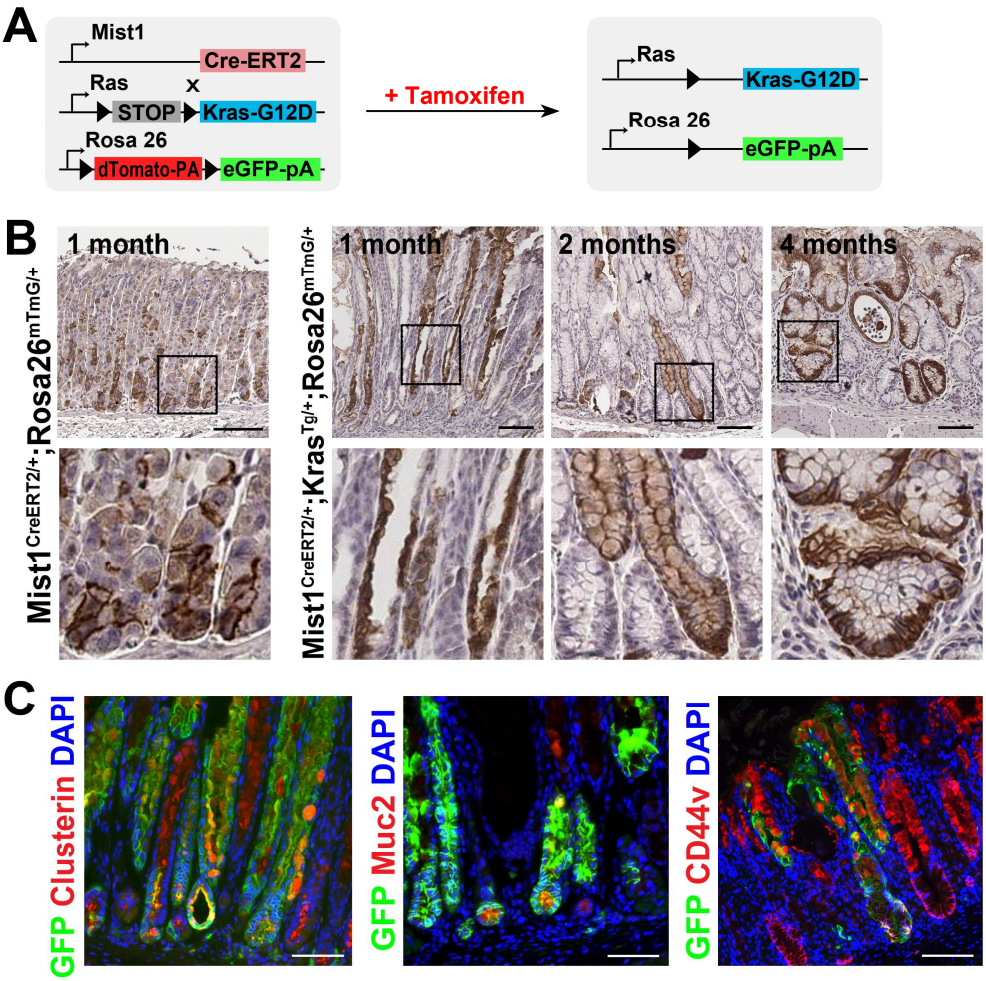
A
Mist1
Cre-ERT2
Ras
x
STOP
Kras-G12D
Rosa 26
dTomato-PA
eGFP-pA
+ Tamoxifen
Ras
Kras-G12D
Rosa 26
eGFP-pA
B
1 month
1 month
2 months
4 months
Mist1CreERT2/+;Rosa26mTmG/+
Mist1CreERT2/+;KrasTg/+;Rosa26mTmG/+
C
GFP Clusterin DAPI
GFP Muc2 DAPI
GFP CD44v DAPI

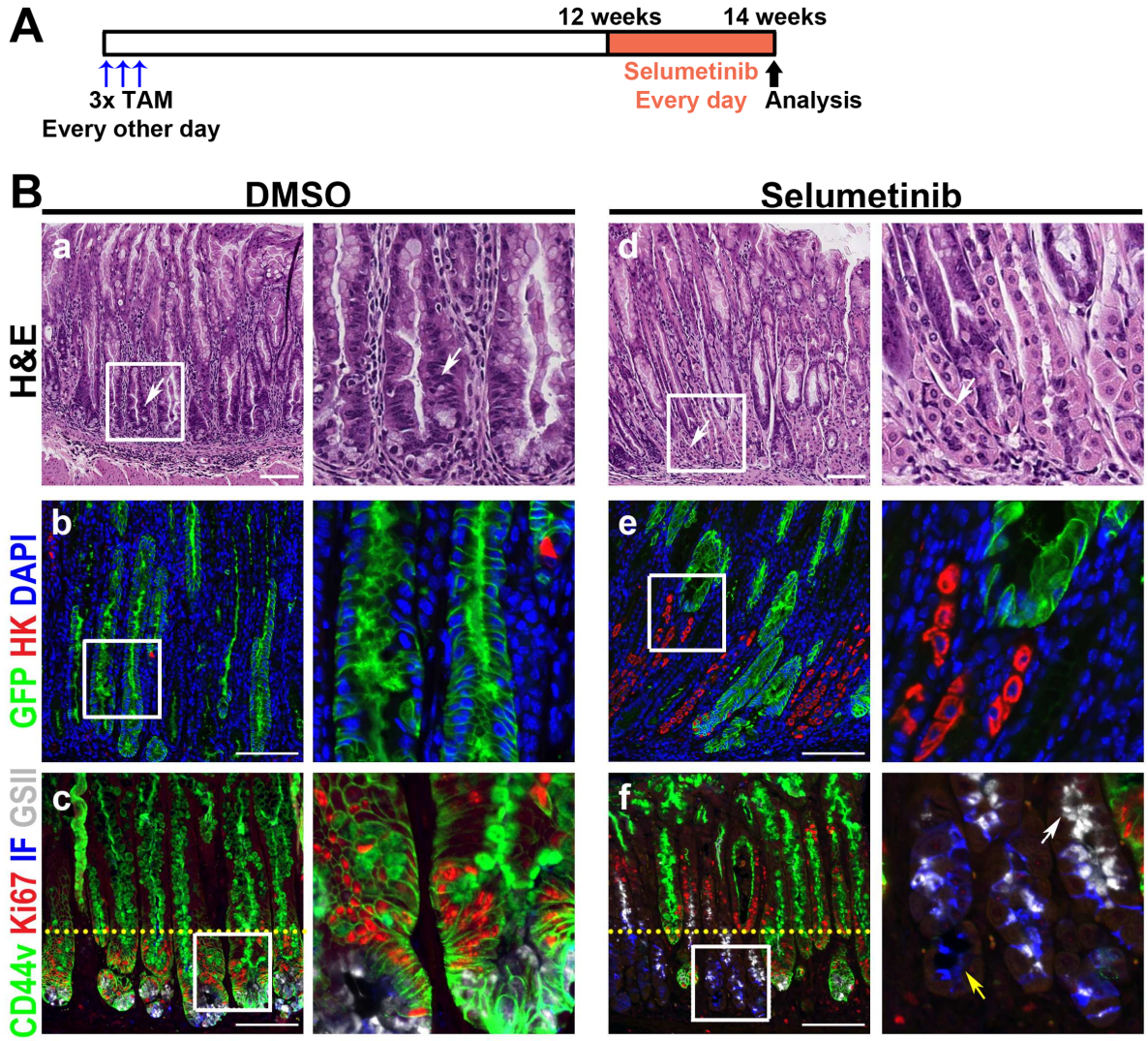
A
12 weeks
14 weeks
3x TAM
Every other day
Selumetinib
Every day
Analysis
B
DMSO
Selumetinib
H&E
GFP HK DAPI
CD44v Ki67 IF GSII
a
b
c
d
e
f

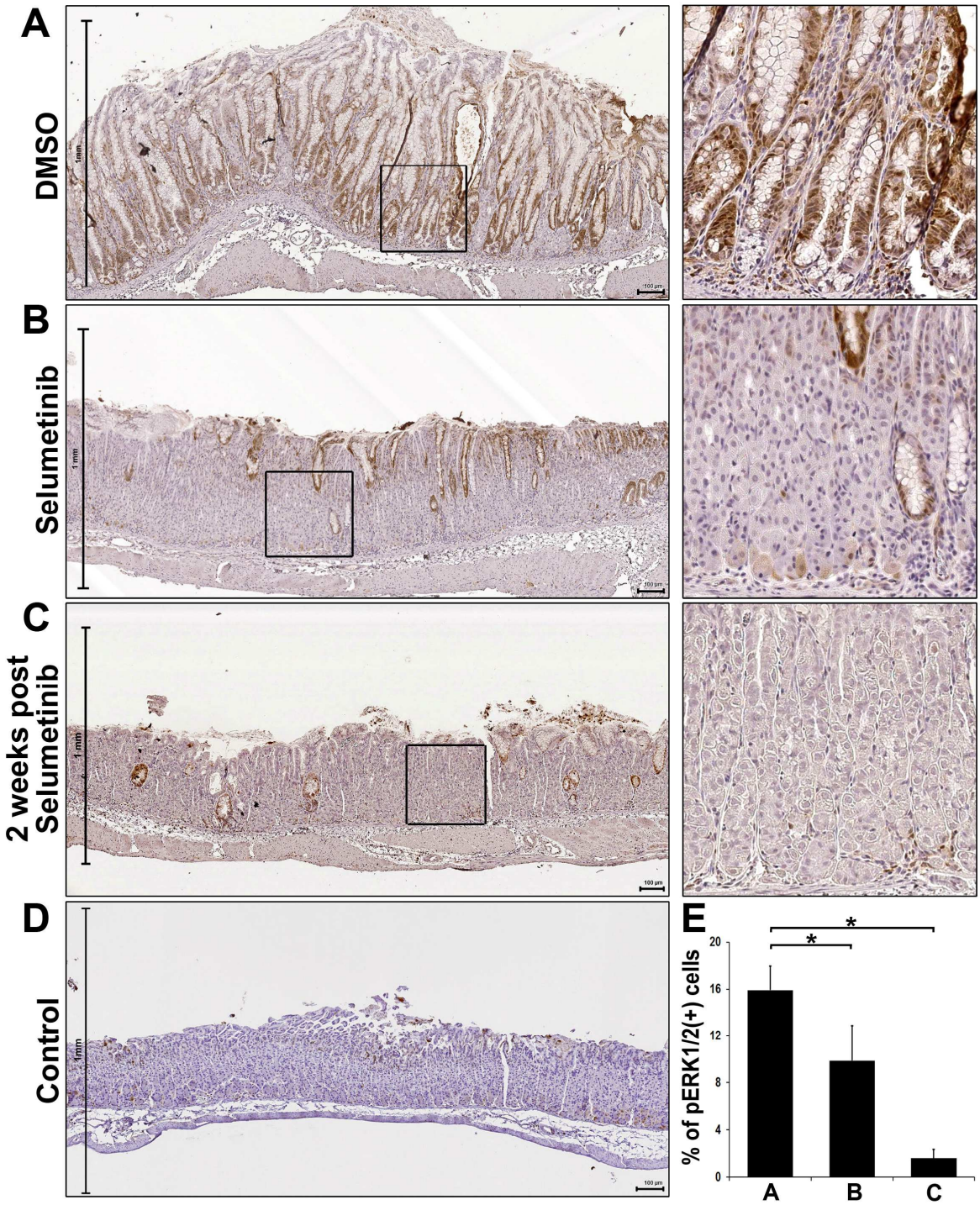
A
DMSO
B
Selumetinib
C
2 weeks post Selumetinib
D
Control
1mm
100 µm
E
% of pERK1/2(+) cells
20
16
12
8
4
0
*
*
A
B
C

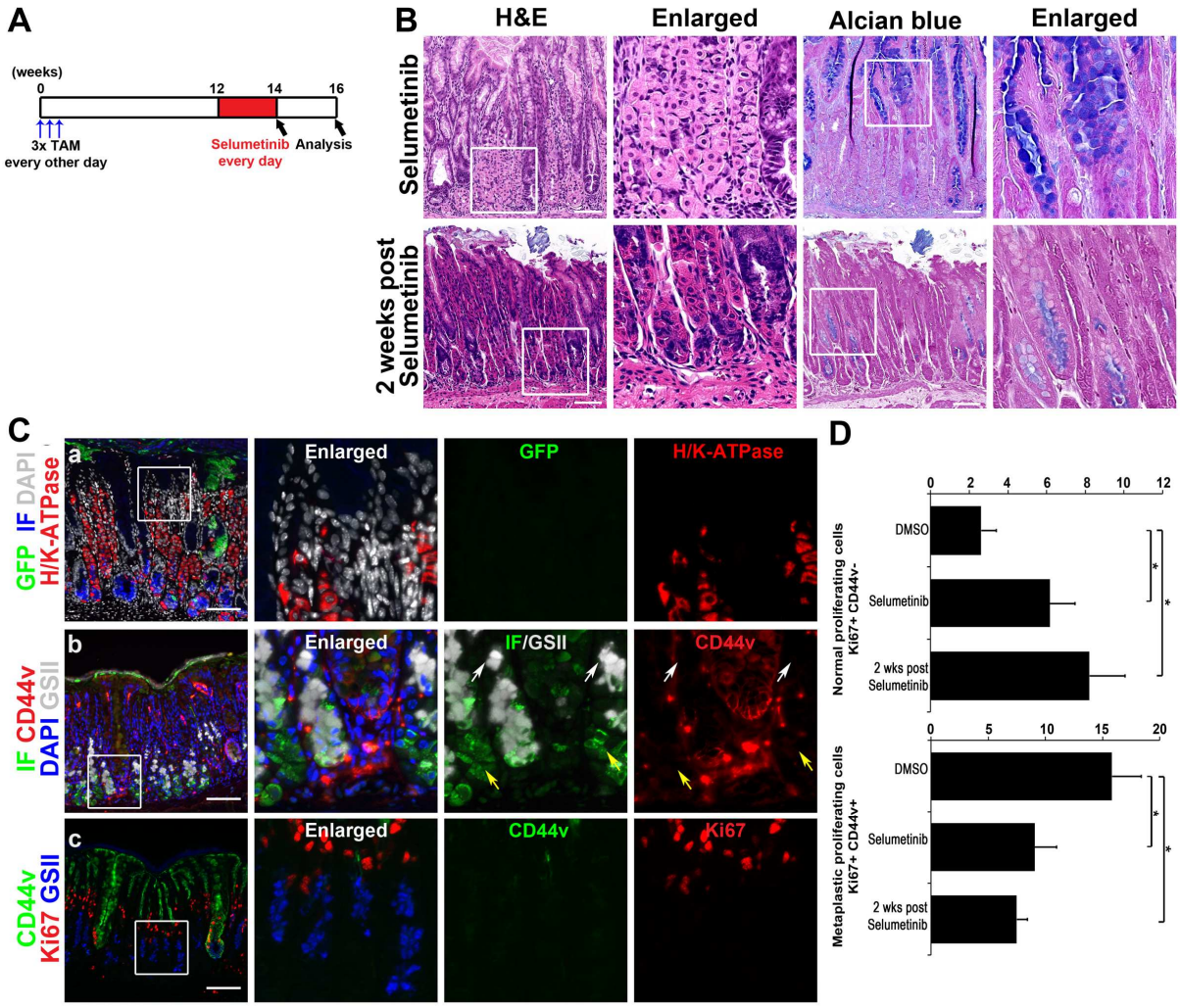
A
(weeks)
0
12
14
16
3x TAM
every other day
Selumetinib
every day
Analysis
B
H&E
Enlarged
Alcian blue
Enlarged
Selumetinib
2 weeks post Selumetinib
C
GFP IF DAPI H/K-ATPase
IF CD44v DAPI GSII
CD44v Ki67 GSII
a
b
c
Enlarged
GFP
H/K-ATPase
IF/GSII
CD44v
Ki67
D
Normal proliferating cells Ki67+ CD44v-
Metaplastic proliferating cells Ki67+ CD44v+
DMSO
Selumetinib
2 wks post Selumetinib
0
2
4
6
8
10
12
5
15
20
*

## SUPPLEMENTAL FIGURE LEGENDS

**Supplemental Figure 1. Histological analysis on the stomach of Mist1-CreERT2 mice after tamoxifen treatment.** A) Sections from Mist1-CreERT2 mouse stomachs (without Kras) at 3 days or 1 week after 3 doses of tamoxifen injection (5 mg subcutaneously) were examined by hematoxylin and eosin (H&E) staining. Normal oxyntic glands were observed in the lesser and greater curvature of the fundic mucosa of stomachs (representative of n=3 (day3) or n=6 (1 week)). Scale bar is 100 µm. B) Quantitative PCR showing relative expression of Atp4a (H/K-ATPase) gene at 3 days after tamoxifen injection. Equal amounts of cDNAs obtained from the lesser and greater curvature of fundus of corn oil or tamoxifen (5 mg subcutaneously, 3 doses) injected Mist1-CreERT2 mouse stomachs were analyzed by real-time PCR using specific primers for Atp4a. For comparisons with the stomach tissue samples, the mean value in corn oil-injected control samples (n=3) was compared with the mean value of tamoxifen-injected mouse samples (n=3). The expression level of H/K-ATPase (Atp4a) gene was not significantly different between samples both from the lesser and greater curvature of the stomachs.

**Supplemental Figure 2. Histological and histochemical analyses on the stomachs of Mist1-Kras mice.** Sections from Mist1-Kras mouse stomachs at 1 week to 4 months after tamoxifen injection were examined by hematoxylin and eosin (H&E) staining, periodic acid–Schiff (PAS) or Alcian blue staining. Metaplastic glands from 1 month post tamoxifen treatment stained with PAS and from 2 months after tamoxifen treatment stained with AB. Arrows indicate PAS- or Alcian blue-positive reactions. Scale bars are 100 µm.

**Supplemental Figure 3. Immunofluorescence staining of phospho-ERK1/2 in Mist1-Kras mouse stomachs. A)** Sections of the oxyntic glands in the corpus from Mist1-Kras mouse stomachs at 1 week after tamoxifen treatment or corn oil treatment (control) were co-immunostained with antibodies against intrinsic factor (IF, green), phospho-ERK1/2 (pERK1/2, red) and GSII-Lectin (GSII, white). Several intrinsic factor-positive chief cells in Mist1-Kras mouse stomachs at 1 week post tamoxifen treatment were co-positive for phospho-ERK1/2 (white arrow). Yellow lines indicate the transition cell zone, which contains co-positive cells for intrinsic factor and GSII-lectin in the lower neck area of oxyntic glands. DAPI was used for nuclear staining (blue). Dotted boxes indicate regions enlarged. Scale bars are 100 μm. B) Quantitation of phospho-ERK1/2 positive cells in Mist1-Kras mouse stomachs at 1 week after tamoxifen injection. Phospho-ERK1/2 positive cells were counted in IF and GSII-lectin dual positive-transition zone cells, or in the IF single positive-chief cells at the bases glands in the corpus of Mist1-Kras mouse stomachs (n=4). * = $p<0.05$.

**Supplemental Figure 4. Histological analysis on the stomachs of Mist1-Kras mice at 1 month after tamoxifen treatment.** Sections from Mist1-Kras mouse stomachs at 1 month after tamoxifen injection were examined by hematoxylin and eosin (H&E) stainin. Arrows indicate parietal cells collapsed at the base of glands. Scale bars are 100 μm.

**Supplemental Figure 5. Immunofluorescence staining of activated Caspase-3 in Mist1-Kras mouse stomachs.** Sections of the oxyntic glands in the corpus from Mist1-Kras mouse stomachs at 1, 2 and 4 weeks after tamoxifen treatment or corn oil treatment (control) were

immunostained with antibodies against cleaved Caspase-3 (green) and H/K-ATPase (red) and observed 50 glands in the corpus (n=3). One cleaved Caspase-3-positive parietal cell was observed only in the Mist1-Kras stomachs at 4 weeks after tamoxifen treatment (white arrow). DAPI was used for nuclear staining (blue). Dotted boxes indicate regions enlarged. Scale bars are 100 μm.

**Supplemental Figure 6. Co-immunostaining of SPEM markers in Mist1-Kras mouse stomachs.** Sections of the glands in the corpus from Mist1-Kras mouse stomachs at 1 week, 1, 2, 3 and 4 months after tamoxifen treatment or corn oil treatment (control) were immunostained with antibodies against Clusterin (green), CD44v (red) and GSII-Lectin (blue). In the Mist1 control mouse stomachs, Clusterin and GSII-Lectin, markers for both mucous neck cells and SPEM, were present in the mucous neck cells of the oxyntic glands in the corpus, however, CD44v, a marker for SPEM, was not observed until at 1 week after tamoxifen treatment. From 1 month after tamoxifen injection, CD44v-positive glands were observed in the corpus of Mist-Kras mouse stomachs and all CD44v-positive glands were co-positive for Clusterin and GSII-Lectin. Dotted boxes indicate regions enlarged. Scale bars are 100 μm.

**Supplemental Figure 7. Immunochemistry of Cdx1 in Mist1-Kras mouse stomachs.** Sections of glands in the gastric body from uninduced wild type mouse stomachs or Mist1-Kras mouse stomachs at 3 months post tamoxifen treatment were immunostained with antibodies against Cdx1. In Mist1-Kras mouse stomachs, Cdx1-expressing cells were observed at the base of metaplastic glands (arrows). The paraffin sections of Mist1-Kras mouse stomachs were also

co-immunostained with antibodies against Cdx1 (red). Cdx1-positive cells were co-positive for Pdx1. DAPI was used for nuclear staining (blue). Scale bars are 100 μm.

**Supplemental Figure 8. Expression of intestinal metaplasia marker transcripts at 3 months after tamoxifen injection.** Quantitative PCR showing relative expression of intestinal metaplasia marker genes at 3 months after tamoxifen injection. Equal amounts of cDNAs obtained from tamoxifen-injected Mist1-mTmG mouse stomachs (Mist1) or Mist1-Kras mouse stomachs (Mist1-Kras) were analyzed by real-time PCR using specific primers for Tff3, Muc2, Cdx1 and Cdx2. For comparisons with the stomach tissue samples, the mean value of Mist1-Kras samples (n=6) were compared with the mean value of Mist1 samples (n=5). * = $p<0.05$.

**Supplemental Figure 9. Co-immunostaining of GFP and Ki67 markers in Mist1-Kras-mTmG mouse stomachs.** A) Sections of the glands in the corpus from Mist1-Kras-mTmG mouse stomachs at 1 week and 1 month after tamoxifen treatment were co-immunostained with antibodies against GFP (green) and Ki67 (red). DAPI was used for nuclear staining (blue). Scale bars are 100 μm. B) Quantitation of proliferating cells in Mist1-Kras-mTmG mouse stomachs. Ki67 and GFP co-positive cells were counted in glands in the corpus from Mist1-Kras-mTmG mouse stomachs at 1 week (n=4) and 1 month (n=3) after tamoxifen injection. * = $p<0.05$.

**Supplemental Figure 10. Immunostaining of phospho-ERK1/2 in human intestinal metaplasia. A)** Human metaplasia tissue array samples were stained with antibodies against phospho-ERK1/2. 91.7% of patient cores (33/36) demonstrated phospho-ERK1/2 staining in the nucleus of mucosal gland cells (arrows). B&C) Human metaplasia tissue array samples were co-stained with antibodies against phospho-ERK1/2, GSII-lectin (SPEM marker) and DMBT1 (IM marker). DAPI was used for nuclear staining (white). B) Phospho-ERK1/2 was positive in SPEM (white arrows) and IM cells (yellow arrow). C) Phospho-ERK1/2 was positive in cells at the transition between SPEM and IM (white arrows). D&E) A serial section of the human metaplasia tissue array samples in B &C was co-stained for phospho-ERK1/2, GSII-lectin (SPEM marker) and Ki67 (proliferation marker). Phospho-ERK1/2 was co-positive for Ki67 in SPEM (white arrows, D), as well as in cells at the transition between SPEM and IM, which expressed and DMBT1 and GSII-lectin (white arrows, E). Boxes indicate regions enlarged. Scale bars = 100 μm.

**Supplemental Figure 11. Immunofluorescence staining of macrophage markers in Mist1-Kras mouse stomachs.** A) CD163-positive macrophages were counted per 20X field of images taken in the corpus from DMSO- or Selumetinib-treated mouse stomachs (n=). * = $p<0.05$.

**Supplemental Figure 12. A model for the development and progression of metaplasia in the Mist1-Kras mouse model.** The composition of metaplastic cells present in the glands representing key metastatic stages from 1 to 4 months post tamoxifen treatment shows the dynamic changes of metaplasia derived from mature chief cells.

**Supplemental table 1. List of primary antibodies**

| MARKER | SPECIES | SOURCE | DILUTION |
|---|---|---|---|
| Clusterin | Goat | Santa Cruz, SC-6420 | 1:2,000 |
| TFF3 | Rabbit | Gift from Daniel K. Podolsky, UT Southwestern | 1:1,000 |
| Intrinsic factor | Goat | Gift from David Alpers, Washington University, St. Louis | 1:2,000 |
| Muc2 | Rabbit | Santa Cruz, SC-15334 | 1:300 |
| Ki-67 | Rat | DAKO, M7249 | 1:300 |
| Lectin GS-II, Alexa Fluor® 647 Conjugate | | Molecular probes, L32451 | 1:2000 |
| CD44v | Rat | Cosmo Bio, LKGM002 | 1:15,000 |
| CD163 | Mouse | NeoMarkers, MS-1103-S0 | 1:300 |
| Ly6B.2 | Rabbit | AbD Serotec, MCA771G | 1:500 |
| F4/80 | Rat | Invitrogen, MF48000 | 1:500 |
| GFP | Chicken | Invitrogen, A10262 | 1:1,000 |
| GFP | Rabbit | Novus, NB600-308 | 1:1,000 |
| Phospho-p44/42 MAPK (Erk1/2) | Rabbit | Cell Signaling, 4370 | 1:1,500 |
| Cleaved Caspase-3 (Asp175) | Rabbit | Cell Signaling, 9661 | 1:300 |
| Cdx1 | Rabbit | Thermo Scientific, PA5-23056 | 1:500 |
| H/K-ATPase | Mouse | Fitzgerald, 10R-H100b | 1:1,000 |
| DMBT1 (g340) | Mouse | Abbiotec LLC, 250390 | 1:500 |
| Human Ki67 | Mouse | VectorLabs, VP-K452 | 1:100 |

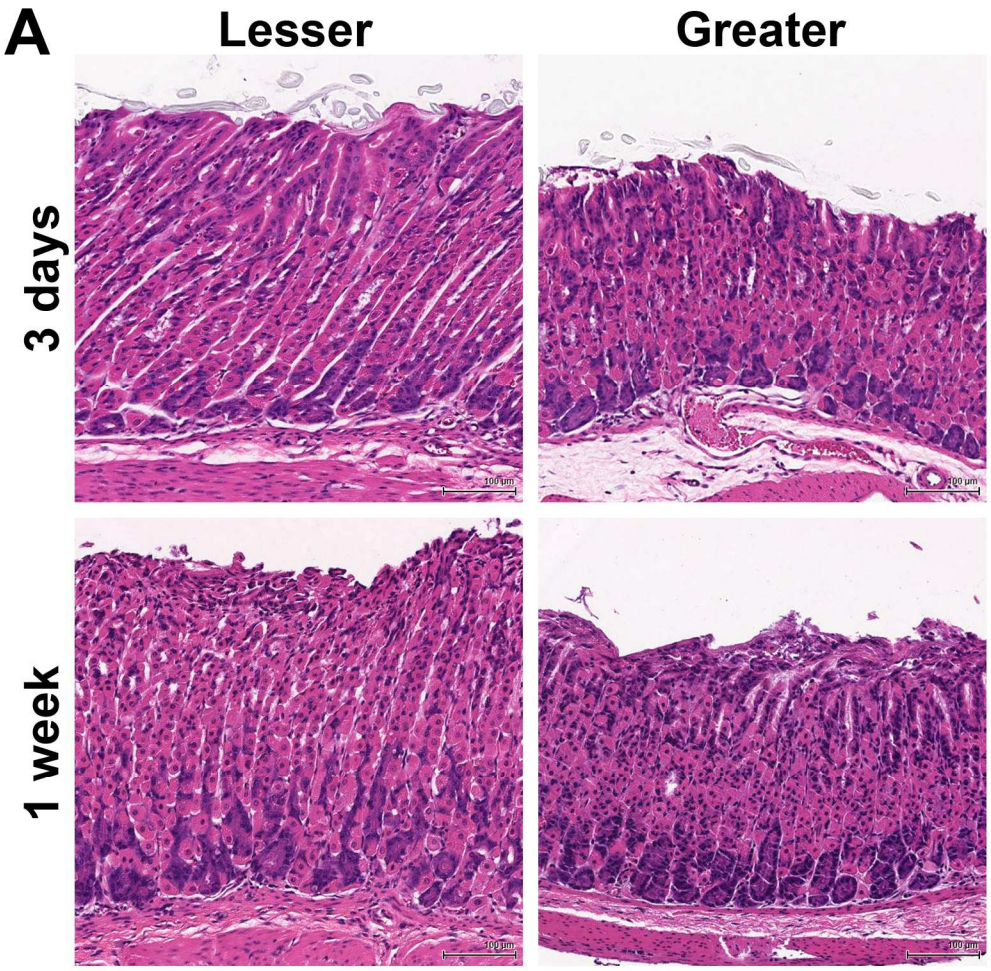
A
Lesser
Greater
3 days
1 week
100 μm

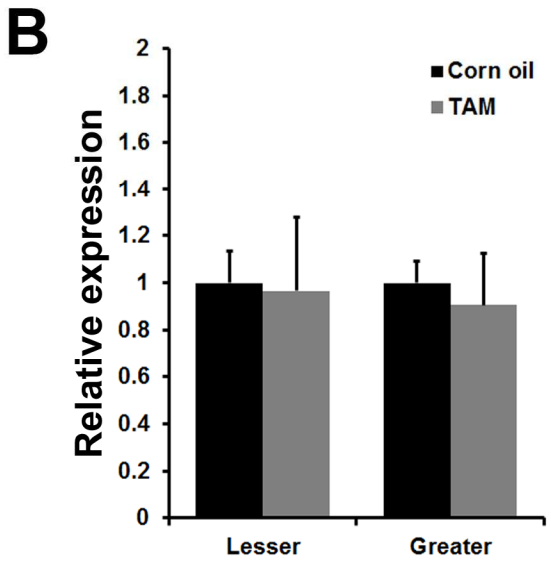
B
Relative expression
2
1.8
1.6
1.4
1.2
1
0.8
0.6
0.4
0.2
0
Corn oil
TAM
Lesser
Greater

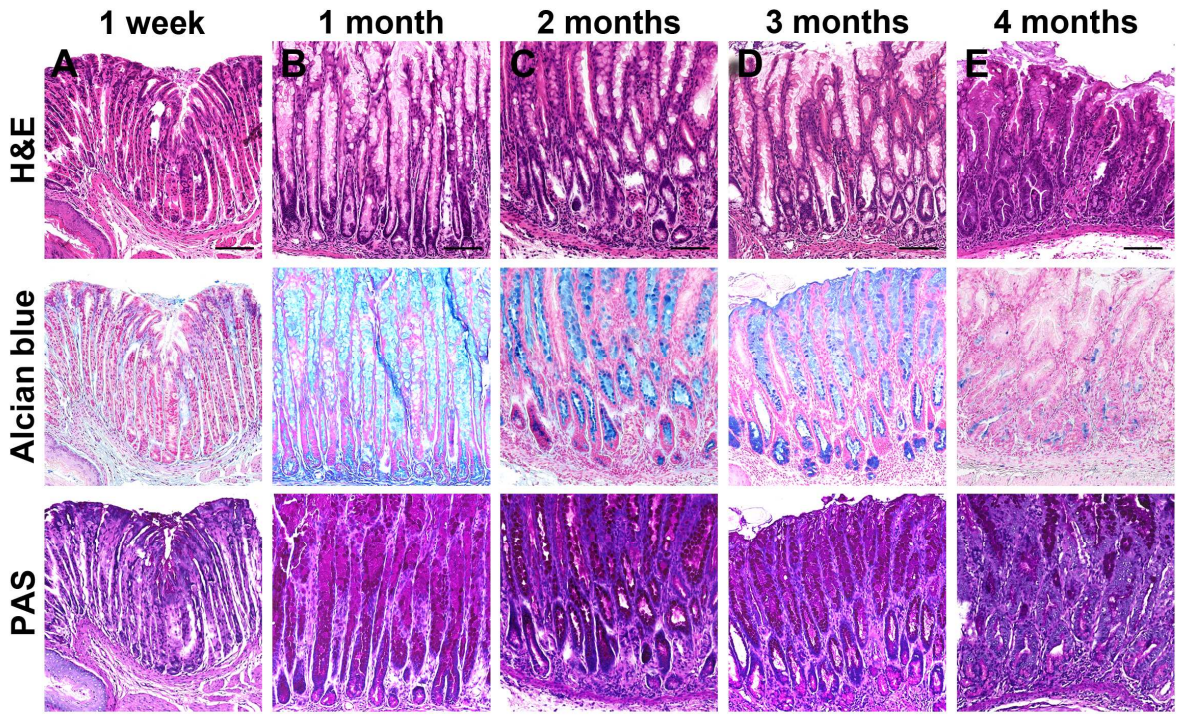
1 week
1 month
2 months
3 months
4 months
A
B
C
D
E
H&E
Alcian blue
PAS

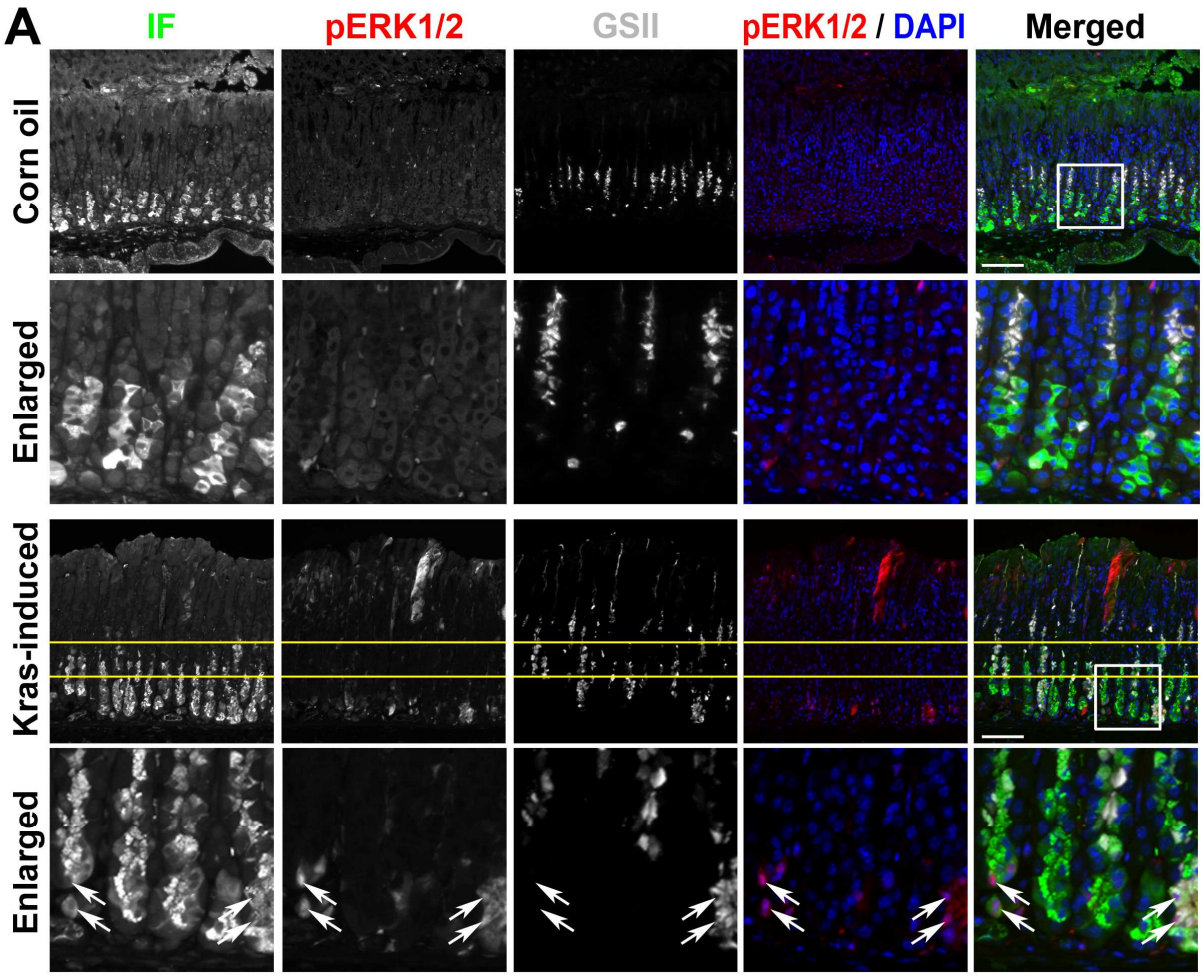
A
IF
pERK1/2
GSII
pERK1/2 / DAPI
Merged
Corn oil
Enlarged
Kras-induced
Enlarged

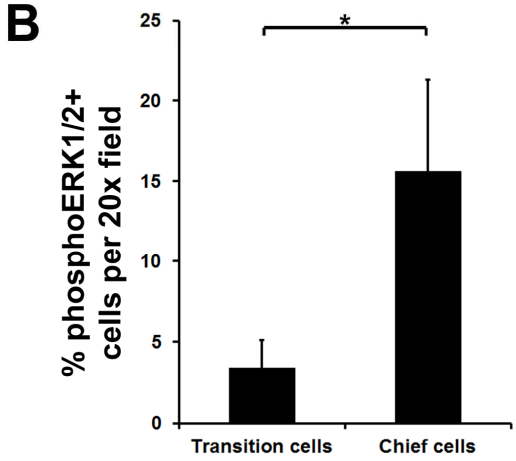
B
*
% phosphoERK1/2+ cells per 20x field
25
20
15
10
5
0
Transition cells
Chief cells

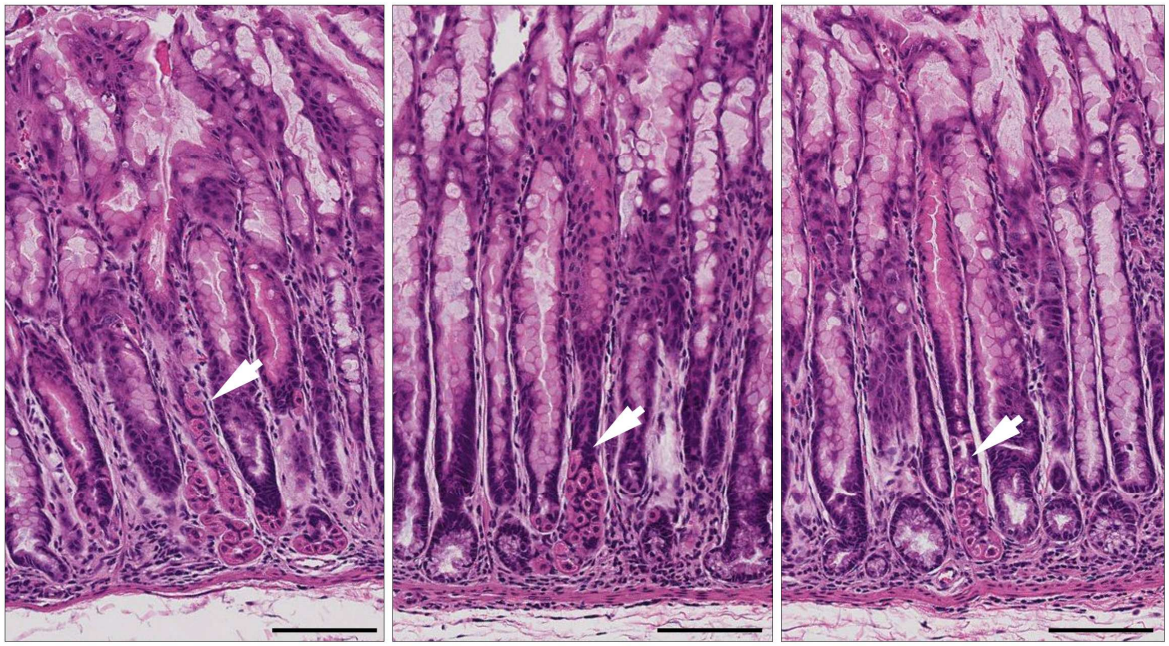

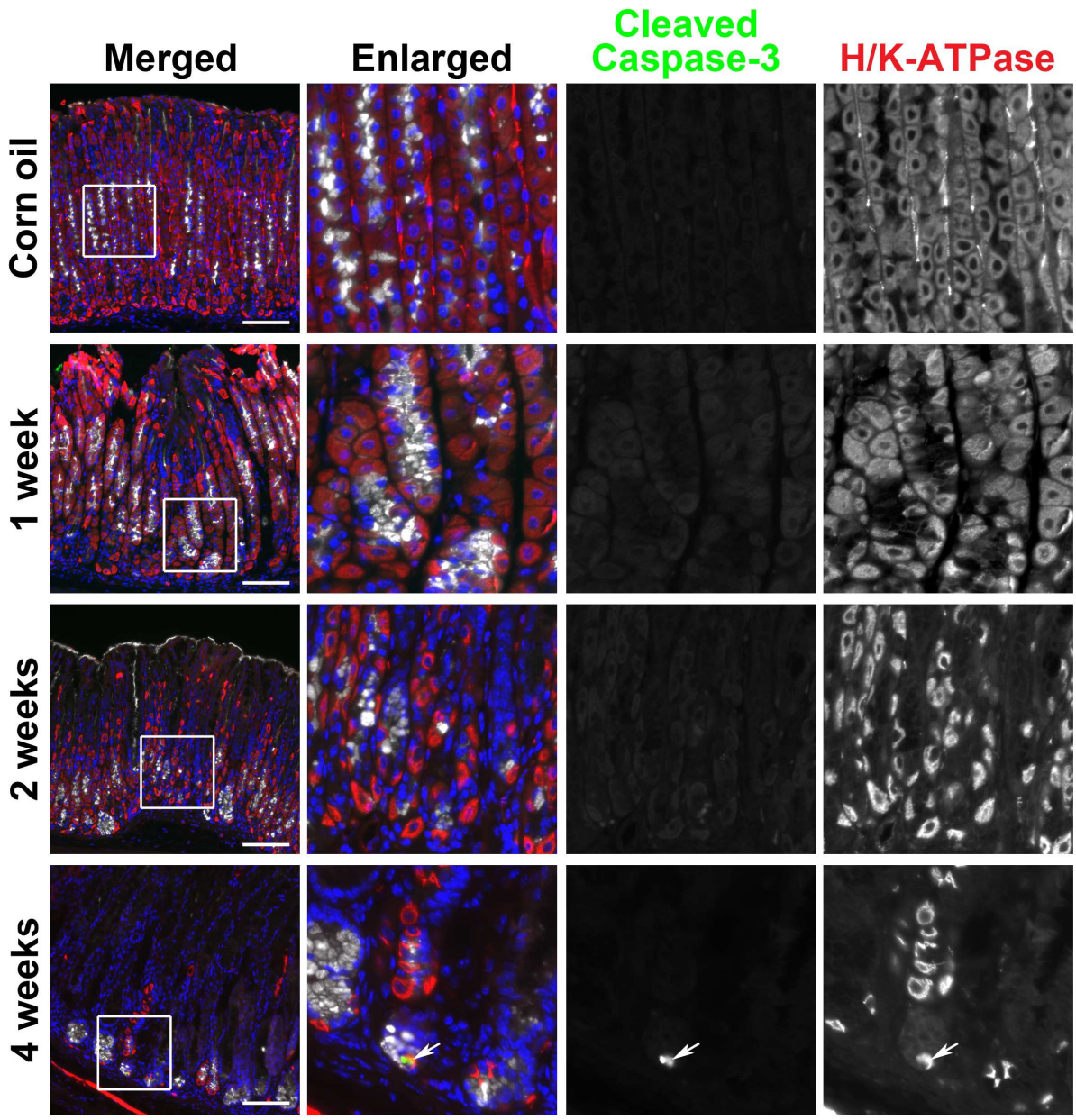
Merged
Enlarged
Cleaved Caspase-3
H/K-ATPase
Corn oil
1 week
2 weeks
4 weeks

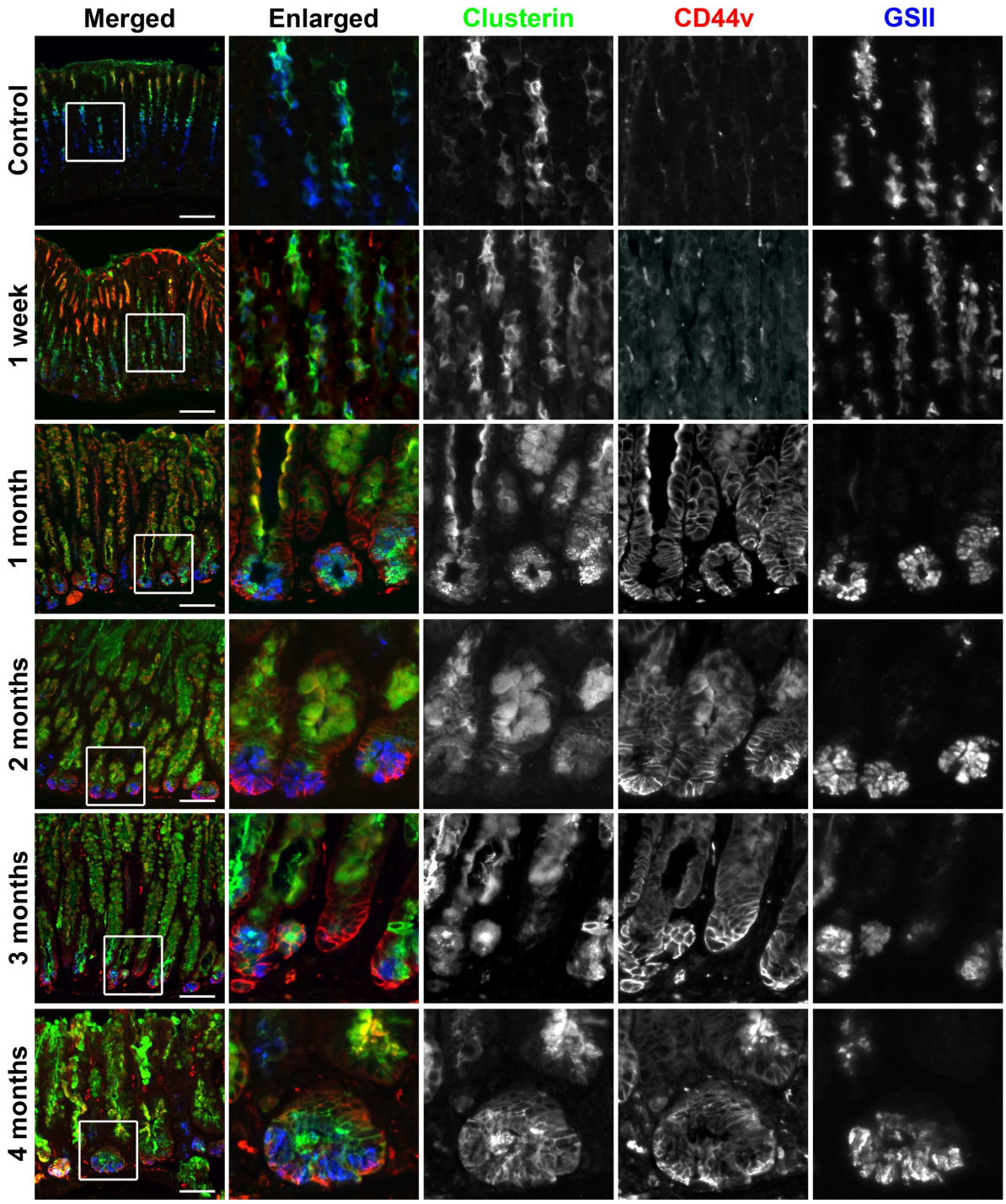
Merged
Enlarged
Clusterin
CD44v
GSII
Control
1 week
1 month
2 months
3 months
4 months

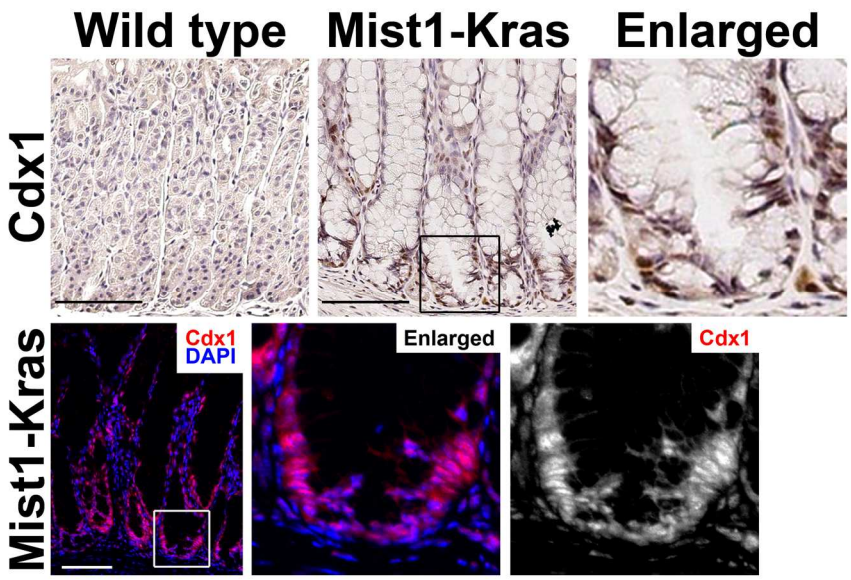
Wild type
Mist1-Kras
Enlarged
Cdx1
Mist1-Kras
Cdx1
DAPI
Enlarged
Cdx1

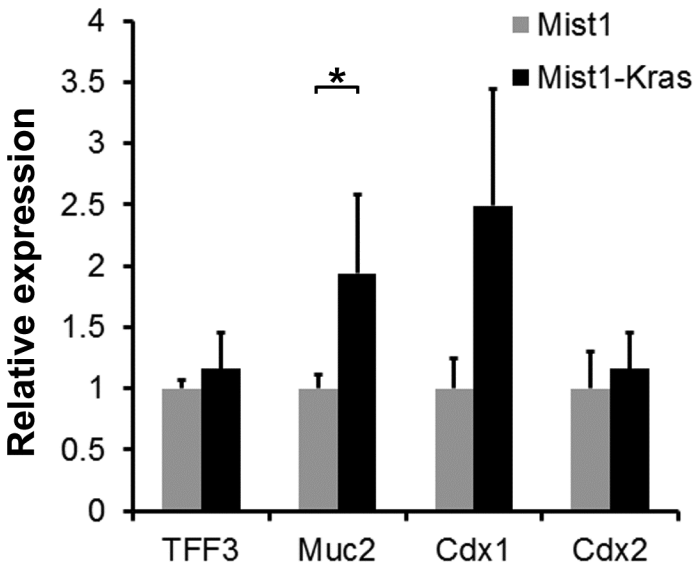
Mist1
Mist1-Kras
Relative expression
4
3.5
3
2.5
2
1.5
1
0.5
0
*
TFF3
Muc2
Cdx1
Cdx2

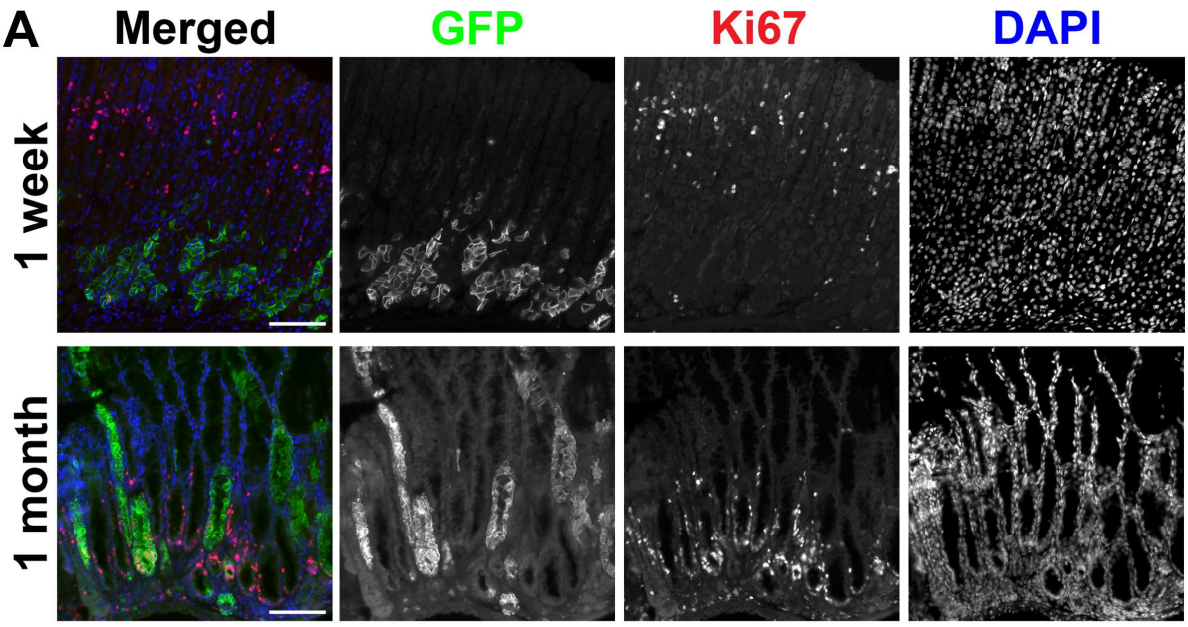
A
Merged
GFP
Ki67
DAPI
1 week
1 month

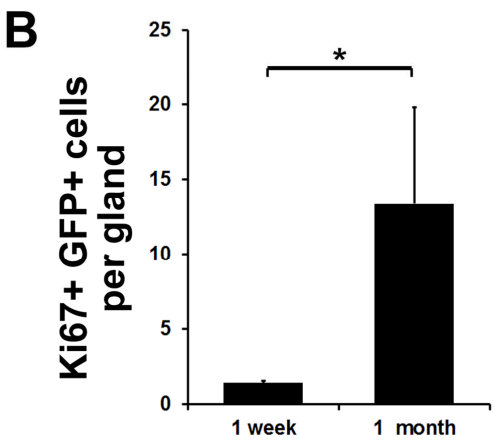
B
Ki67+ GFP+ cells per gland
25
20
15
10
5
0
*
1 week
1 month

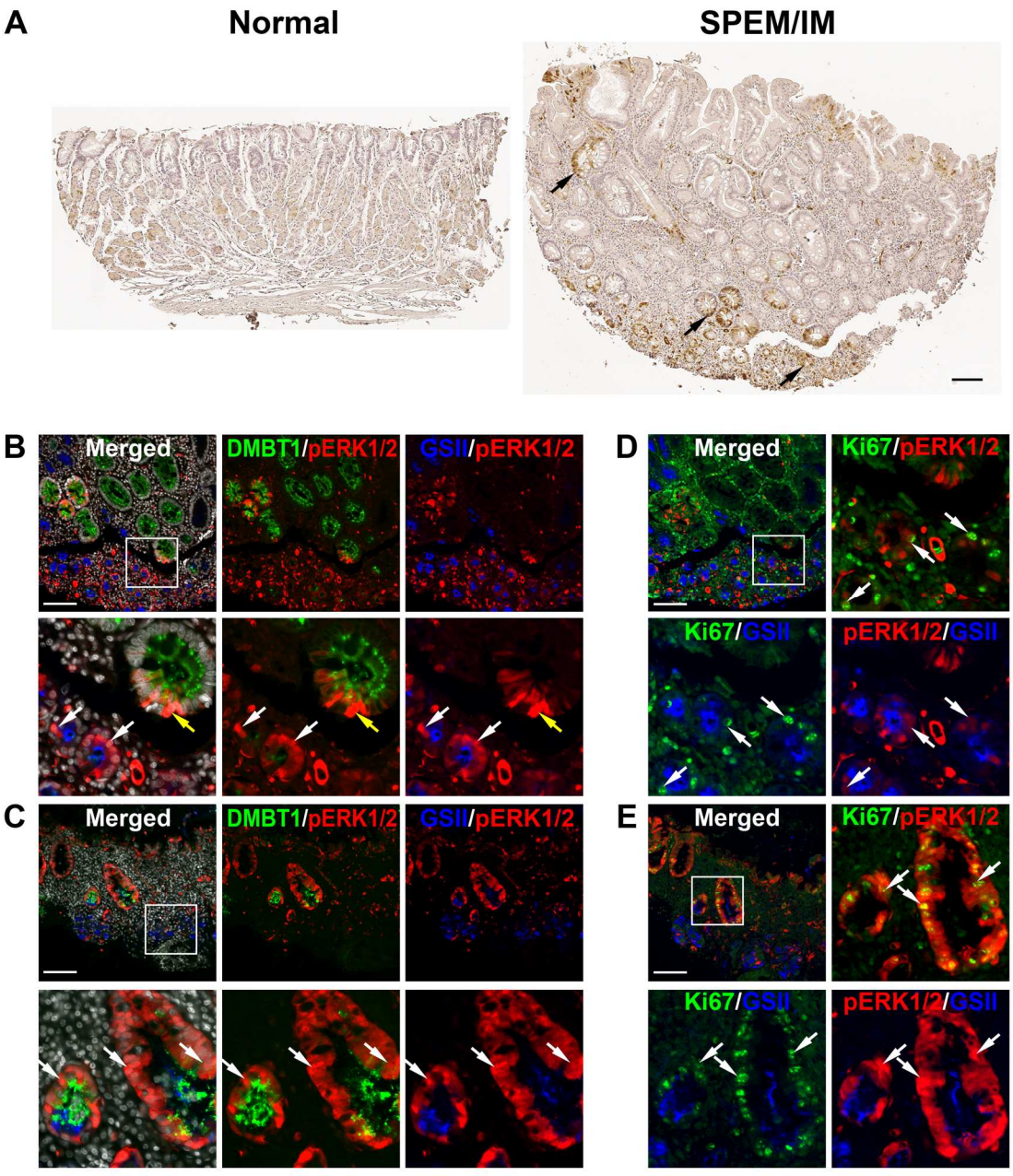
A
Normal
SPEM/IM
B
Merged
DMBT1/pERK1/2
GSII/pERK1/2
C
Merged
DMBT1/pERK1/2
GSII/pERK1/2
D
Merged
Ki67/pERK1/2
Ki67/GSII
pERK1/2/GSII
E
Merged
Ki67/pERK1/2
Ki67/GSII
pERK1/2/GSII

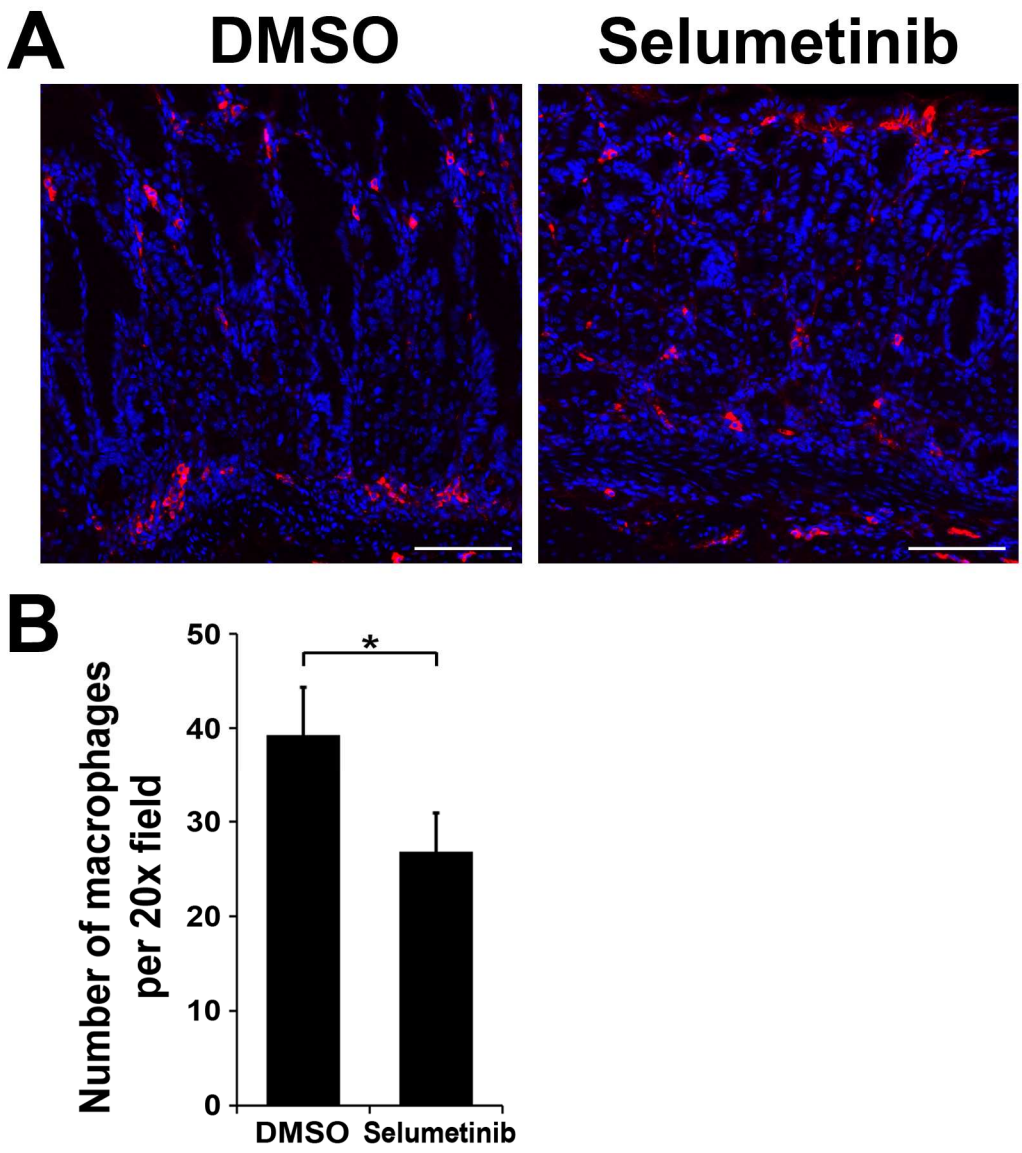
A
DMSO
Selumetinib
B
Number of macrophages per 20x field
50
40
30
20
10
0
*
DMSO
Selumetinib

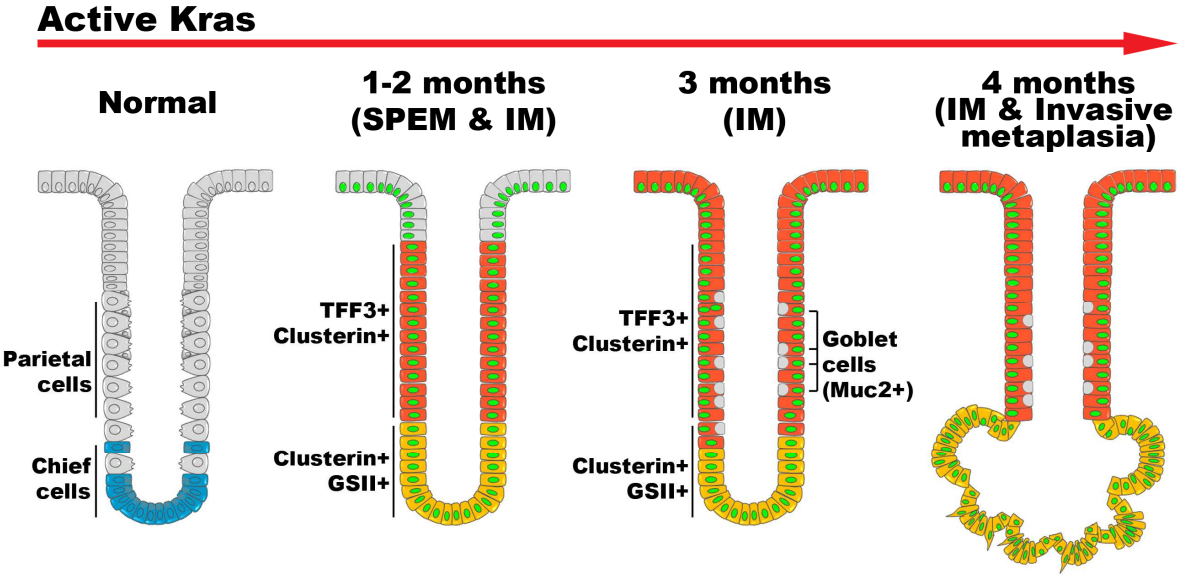
Active Kras
Normal
1-2 months
(SPEM & IM)
3 months
(IM)
4 months
(IM & Invasive
metaplasia)
Parietal
cells
Chief
cells
TFF3+
Clusterin+
Clusterin+
GSII+
TFF3+
Clusterin+
Goblet
cells
(Muc2+)
Clusterin+
GSII+